Energetics of BCM type synaptic plasticity and storing of accurate information

Jan Karbowski[1,2]

[1] *Institute of Applied Mathematics and Mechanics, University of Warsaw, ul. Banacha 2, 02-097 Warsaw, Poland;*

[2] *Nalecz Institute of Biocybernetics and Biomedical Engineering, Polish Academy of Sciences, 02-109 Warsaw, Poland*

Abstract

Excitatory synaptic signaling in cortical circuits is thought to be metabolically expensive. Two fundamental brain functions, learning and memory, are associated with long-term synaptic plasticity, but we know very little about energetics of these slow biophysical processes. This study investigates the interplay between stochastic BCM type synaptic plasticity, its metabolic requirements, and the accuracy and retention of stored information in synaptic weights, within the frameworks of stochastic dynamical systems and nonequilibrium thermodynamics. The dynamic mean-field is derived for the synaptic weights, and it is found that the energy used by plastic synapses, related to their information content, is primarily caused by fluctuations in the synaptic weights and in presynaptic firing activity. Such information-related plasticity energy rate, together with the accuracy of stored information depend nonlinearly on key neurophysiological parameters, which is due to bistability in the system: synapses plus their postsynaptic neuron. At the onset of bistability, the memory lifetime, its accuracy, and plasticity energy rate are all positively correlated and exhibit sharp peaks. However, in the bistable regime, the accuracy of encoded information and plasticity energetics are generally anticorrelated, which suggests that a precise storing of synaptic information neither has to be metabolically expensive nor it is limited by energy consumption. Interestingly, such a limit on synaptic coding accuracy is imposed instead by a derivative of the plasticity energy rate with respect to the presynaptic firing, and this relationship has

a general character that is independent of the plasticity type. An estimate for primate neocortex reveals that a relative metabolic cost of BCM type synaptic plasticity, as a fraction of the overall neuronal cost, can vary from negligible to substantial, depending on a synaptic working regime and presynaptic firing.

Email: jkarbowski@mimuw.edu.pl

Keywords: energy cost of synaptic plasticity; accurate storing of synaptic information; bistability; memory lifetime; metabolism; thermodynamic limits on memory.

1. Introduction

Information and energy are intimately related for all physical systems because information has to be written on some physical substrate which always comes at some energy cost [1, 2, 3, 4, 5]. Brains are physical devices that process information and simultaneously dissipate energy [6, 7] in the form of heat [8]. This energetic cost is relatively high [7, 9, 10, 11], which is the likely cause for a sparse coding strategy in neural circuits [12, 13]. Experimental studies [14, 15], as well as theoretical calculations based on data [16, 17], indicate that short-term synaptic signaling is the major consumer of metabolic energy.

Brains are also highly adapting objects, which learn and remember by encoding and storing long-term information in excitatory synapses (dendritic spines) [18, 19]. These important slow processes are driven by correlated electric activities of pre- and postsynaptic neurons [20, 21, 22, 23, 24] and cause plastic modifications in spine's intrinsic molecular machinery, leading to changes in spine size, its conductance (weight) and postsynaptic density (PSD) [18, 25, 26, 27]. Consequently synaptic plasticity and associated information writing and storing must cost energy, since spines require chemical energy for maintaining AMPA and NMDA receptors [28, 29], as well as for powering various molecular processes associated with PSD [30, 31]. The most visible empirical manifestation of the plasticity-energy relationship is present for mammalian cortical development, during which synaptic density can change several fold and strongly correlates with changes in glucose metabolic rate of cortical tissue [17]. Unfortunately, despite a massive literature on modeling synaptic plasticity (e.g. [21, 22, 23, 24, 32, 33,

34, 35, 36, 37, 38, 39, 40, 41, 42, 43, 44]), our theoretical understanding of the energetic requirements underlying synaptic plasticity and memory storing is currently lacking. In particular, we do not know the answers to the basic questions, such as how does energy consumed by plastic synapses depend on key neurophysiological parameters, and more importantly, whether energy restricts the precision of synaptically encoded information and its lifetime, and to what extent. Such a knowledge might lead to a deeper understanding of two fundamental problems in neuroscience: one related to the physical cost and control of learning and memory in the brain [18, 19, 30, 37, 45, 46, 47], and another more practical related to dissecting the contribution of synaptic plasticity to signals in brain imaging [10, 14, 48, 49]. A recent study by the author [50] provided some answers to the above questions, by analysing molecular data in synaptic spines and by modeling energy cost of learning and memory in a cascade model of synaptic plasticity (mimicking molecular interactions in spines). From that study it follows that the average cost of synaptic plasticity constitutes a small fraction of the metabolic cost used for fast excitatory synaptic transmission, about $4-11\%$, and that storing longer memory traces can be relatively cheap [50]. However, this study left open other questions, e.g., how does the energy cost of synaptic plasticity depend on neuronal firing rates, synaptic noise, and other neural characteristics, and what is the relationship between such energy cost and a precise storing of synaptic information?

The main goal of this study is to uncover a relationship between synaptic plasticity, its energetics, and a precise information storing at excitatory synapses for one of the best known forms of synaptic plasticity due to Bienenstock, Cooper, and Munro, the

so-called BCM rule [21]. This is a different (more macroscopic) but a complementary level of modeling to the one (microscopic) in [50]. Specifically, we want to find the energy cost of maintaining an accurate information at synapses in the face of ongoing variable neural activity and thermodynamic fluctuations inside spines associated with variation in the number of membrane receptors. The phenomenological BCM rule has been shown to explain several key experimental observations [51], and it is equivalent to a more microscopic STDP rule [20, 23, 24] under some very general conditions [34, 52]. Since, the BCM rule is believed to describe initial phases of learning and memory [47], the focus of this work is on the energy cost and coding accuracy of the early synaptic plasticity, i.e. early long-term potentiation (e-LTP) and depression (e-LTD), which lasts from minutes to several hours. We do not consider explicitly the effects of memory consolidation that operate on much longer time scales and which are associated with late phases of LTP and LTD (l-LTP and l-LTD) [40, 42, 53]. However, we do provide a rough estimate of the energetics of these late processes, and they turn out to be much less energy demanding than the early phase plasticity.

One can question whether the approach taken here, with the macroscopic BCM type model, is reasonable for modeling and calculating energy cost of synaptic plasticity? Maybe a more microscopic approach should be used with explicit molecular interactions between PSD proteins? However, the basic problem with such a microscopic more detailed approach is that we do not know most of the molecular signaling pathways in a dendritic spine, we do not know the rates of various reactions, and even the basic mechanism of encoding information at synapses is unclear. For example, for a long time

it was thought that CaMKII persistent autophosphorylation provides a basic mechanism of information storage via bistability [30, 31]. However, experimental data indicate that CaMKII enhanced activity after spine activation is transient and lasts only about 2 min [54], which casts doubts on its persistent enzymatic activity and its role as a "memory molecule" (for a review see [55]). Taking all these uncertainties into account, it seems that more macroscpic approach might be more reliable, at least partly.

Because synapses/spines are small, they are strongly influenced by thermal fluctuations [18, 29, 56]. For this reason, this paper uses universal methods of stochastic dynamical systems and non-equilibrium statistical mechanics [57, 58, 59, 60, 61, 62, 63, 64]. The latter are generally valid for all physical systems, including the brain, operating out of thermodynamic equilibrium. Regrettably, the methods of non-equilibrium thermodynamics have virtually not been used in neuroscience despite their large potential in linking brain physicality with its information processing capacity, with two recent exceptions [50, 65]. (This should not be confused with equilibrium thermodynamics, whose methods have occasionally been used in neuroscience, although in a different context, e.g., [12, 66, 67].)

General outline of the problem considered.

It is generally believed that long-term information in excitatory synapses is encoded in the pattern of synaptic strengths or weights (membrane electric conductance), which is coupled to the molecular structure of postsynaptic density within dendritic spines [19, 30, 31, 45, 68]. This study considers the energy cost associated with maintaining the pattern of synaptic weights. In particular, we analyze the energetics and information

capacity of the fluctuations in the number of AMPA and NMDA receptors on a spine membrane, or equivalently, fluctuations in the synaptic conductance. Such a variability in the receptor number tends to spread the range of synaptic weights (affecting their structure and distribution) that has a negative consequence on the encoded information and can lead to its erasure. In terms of statistical mechanics, the receptor fluctuations increase the entropy associated with the distribution of synaptic weights, and that entropy has to be reduced to preserve the information encoded in the weights. This very process of reducing the synaptic entropy production is a nonequilibrium phenomenon that costs some energy, which has to be provided by various processes involving ATP generation [57].

The BCM type of synaptic plasticity used here is a phenomenological model that does not relate in a straightforward way to the underlying synaptic molecular processes. Empirically speaking, a change in synaptic weight in e-LTP is caused by a sequence of molecular events, of which the main are: activation of proteins in postsynaptic density, which subsequently stimulates downstream actin filaments elongation (responsible for a spine enlargement), and AMPA and NMDA receptor trafficking [28, 29]. Therefore, it is assumed here that BCM-type rule used here macroscopically reflects broadly these three microscopic processes, especially the first and the last. (Spine volume related to actin dynamics is not explicitly included in the model, although it is known experimentally that spine volume and conductance are positively correlated [18].) Thus, it is expected that the synaptic energy rate calculated here is related to ATP used mainly for postsynaptic protein activation (through phosphorylation process [68]) and recep-

tor insertion and movement along spine membrane. Obviously, there are many more molecular processes in a typical spine, but they are either not directly involved in spine conductance variability or they are much faster than the above processes (e.g. releasing Ca^{2+} from internal stores is fast). A detailed empirical estimation based on molecular data suggests that protein activation via enhanced phosphorylation is the dominant contribution to the energy cost (ATP rate) of synaptic plasticity [50]. Therefore, the theoretical energy rate of synaptic plasticity determined here should be viewed as a minimal but a reasonable estimate of energetic requirement of LTP and LTD, and it is strictly associated with the information encoded in synaptic weights.

Experimental data show that excitatory synapses can exist in two or more stable states, characterized by discrete synaptic weights or sizes [18, 69, 70, 71, 72, 73]. Data on a single synapse level indicate that synapses can operate as binary elements either with low or high electric conductance [70, 71]. On the other hand, the data on a population level, more relevant to this work, show that synapses can assume more than two stable discrete states [18, 72, 73]. In either case, the issue of bistability vs. multistability is not yet resolved. In this study, a minimal scenario is considered in which synapses together with its postsynaptic neuron can effectively act as a binary coupled system, characterized by a single variable, which is the mean-field postsynaptic current with one or two stable states. The bistability is produced here on a population level from an extended BCM model, which in principle allows for continuous changes in synaptic weights for the individual synapses. The important point is that these continuous weights are correlated, due to plasticity constraints, and thus converge on a mean-field

population level either to one or to a couple of stable values.

Synaptic plasticity processes are induced by a correlated firing in pre- and post-synaptic neurons, and thus a model of neuron activity is also needed. This study uses a firing rate neuron model of the so-called class one nonlinear firing rate curve, which is believed to be a good approximation to biophysical neuronal models [74, 75]; see the Methods for details.

The paper is organized as follows. First, we derive an effective equation for the mean-field stochastic dynamics of the synaptic currents starting from the BCM plasticity rule. Then, we translate this effective equation into probabilistic Fokker-Planck formalism, and derive an effective steady-state potential for the synaptic current. With the help of the effective potential we find entropy production and Fisher information associated with the synaptic plasticity stochastic dynamics. Entropy production is related to the energy cost of BCM plasticity, while the Fisher information is related to the accuracy of encoded information in synapses (strictly in the mean-field synaptic current) about the presynaptic input. Details of the calculations are provided in the Methods (and some in Supporting Information S1).

2. Results

Effective equation for stochastic BCM-like synaptic plasticity: separation of time scales.

In this section an effective equation for population averaged synaptic current is derived, starting from the BCM plasticity rule. This single mean-field synaptic equation will be much easier to handle analytically than many coupled equations describing the dynamics of the system of many synapses on a typical neuron.

We consider a sensory neuron with N plastic excitatory synapses (dendritic spines). We assume that synaptic weights w_i $(i = 1, ..., N)$, corresponding to spine electric conductances, change due to two factors: correlated activity in presynaptic and post-synaptic firing rates (f_i and r, respectively), and thermodynamic fluctuations in spine conductance ($\sim \sigma_w$). The latter are caused by an internal thermal noise present in spines because of their small size (< 1 μm) and relatively small number of molecular components [18, 56]. The dynamics of synaptic weights is given by a modified BCM plasticity rule [21]:

$$\frac{dw_i}{dt} = \lambda f_i r(r-\theta) - \frac{(w_i - \epsilon a)}{\tau_w} + \frac{\sqrt{2}\sigma_w(\tau_f f_i)^z}{\sqrt{\tau_w}}\eta_i \tag{1}$$

$$\tau_\theta \frac{d\theta}{dt} = -\theta + \alpha r^2, \tag{2}$$

where λ is the amplitude of synaptic plasticity controlling the rate of change of synaptic conductance, τ_w is the weights time constant controlling their decay duration, θ is the

homeostatic variable the so-called sliding threshold (adaptation for plasticity) related to an interplay of LTP and LTD with time constant τ_θ, and α is the coupling intensity of θ to the postsynaptic firing rate r. The parameter σ_w is the standard deviation of weights (in units of conductance) due to stochastic intrinsic fluctuations in spines, which are represented as Gaussian white noise η_i with zero mean and Delta function correlations, i.e., $\langle \eta_i(t) \rangle_\eta = 0$ and $\langle \eta_i(t)\eta_j(t') \rangle_\eta = \delta_{ij}\delta(t-t')$ [58]. For the thermal noise we consider two exclusive cases: either noise amplitude is independent of the presynaptic firing rate f_i ($z = 0$) or it is proportional to f_i ($z = 1$). The time scale τ_f of fluctuations in f_i was added in the noise term to maintain the dimensionality of σ_w in units of conductance. Finally, the product ϵa is the minimal synaptic weight when there is no presynaptic stimulation ($f_i = 0$), where the unitless parameter $\epsilon \ll 1$. There are two modifications to the conventional BCM rule: the stochastic term $\sim \sigma_w$, and the decay term of synaptic weights with the time constant τ_w, which is key for reproducing a binary nature of synapses [70, 71] and for determining energy used by synaptic plasticity.

The conventional BCM rule (i.e. for $\tau_w \mapsto \infty$ and $\sigma_w = 0$) describes temporal changes in synaptic weights due to correlated activity of pre- and post-synaptic neurons (both f_i and r are present on the right in Eq. (1)). These activity changes can either increase the weight, if postsynaptic firing r is greater than the sliding threshold θ (this corresponds to LTP), or they can decrease the weight if $r < \theta$ (corresponding to LTD). The interesting aspect is that θ is also time dependent, and it responds quickly to changes in the postsynaptic firing. In effect, when both dynamical processes in Eqs.

(1-2) are taken into account, the synapse is potentiated for low r (LTP) and depressed for high r (LTD).

The stochastic system of $N+1$ equations described by Eqs. (1) and (2) is intractable analytically, because it is a coupled nonlinear system. The coupling takes place via postsynaptic firing rate r, which depends on all synaptic weights w_i. Therefore, the first goal is to reduce this multidimensional system into a single effective equation that would be amenable to analytical considerations, and which enable us to obtain explicit formulae for synaptic energy rate and coding accuracy. Such reduction can be done because of the time scale separation between neural firing dynamics (changes typically on the order of seconds or less) and between synaptic plasticity (changes on the timescale of minutes/hours). Moreover, we assume that the two synaptic plasticity processes, described by Eqs. 1 and 2, have two distinct time scales, and the dominant is τ_w. This is in agreement with empirical observations and estimations, since τ_w must be of the order of 1 hr to be consistent with slice experiments, showing wiping out synaptic potentiation after about 1 hr when presynaptic firing becomes zero [76, 77]. (Note that τ_w refers to the decay of synaptic weights to the baseline value ϵa, and it should not be confused with a characteristic time of plasticity induction, which is controlled by the product $\lambda f_i r$ in Eq. (1) and which can be much faster, $\sim$ minutes [70, 71].) On the other hand, the time constant τ_θ must be smaller than about 3 min for stability reasons [47, 77], and it even has been estimated as small as $\sim$ 12 sec [78]. Consequently, for times of the order of τ_w, we have $d\theta/dt \approx 0$, which implies that $\theta \approx \alpha r^2$. The details of the reduction procedure can be found in the Methods, and we obtain a single plasticity

equation for a population averaged excitatory postsynaptic current v per spine, which is related to w_i and f_i by $v \sim (1/N)\sum_i f_i w_i$. The result is

$$\frac{dv}{dt} = hr^2(1-\alpha r) - (v - \epsilon c f_o)/\tau_w + \frac{\sqrt{2}\sigma_v}{\sqrt{\tau_w}}\overline{\eta}. \tag{3}$$

This equation essentially couples slow synaptic activities with fast neural activities, and gives a single equation describing the mean-field dynamics of the coupled system: synapses plus their postsynaptic neuron. In Eq. (3), the symbol h is the driving-plasticity parameter given by

$$h = \lambda\beta(f_o^2 + \sigma_f^2), \tag{4}$$

with f_o and σ_f denoting the mean and standard deviation of presynaptic firing rates, and β depending on neurophysiological parameters related to synaptic currents as $\beta = q|V_r|(\tau_{nmda} + \tau_{ampa})$, where q is the probability of neurotransmitter release, V_r is the neuron resting membrane potential, and τ_{nmda}, τ_{ampa} are the time constants for NMDA and AMPA receptors (see the Methods for details). Mathematically, the driving-plasticity h is proportional to the product of plasticity amplitude λ and the presynaptic driving $(f_o^2 + \sigma_f^2)$, which implies that h grows quickly with the presynaptic firing rate. Physically, h is proportional to the electric charge that, on average, can enter the spine due to a correlated activity of pre- and post-synaptic neurons (h has a unit of electric charge). This means that the magnitude of h is a major determinant of the plasticity

(driving force counteracting the synaptic decay), since larger h can experimentally correspond to more Ca^{+2} entering the spine and a higher chance of invoking a change in synaptic strength, which agrees qualitatively with the experimental data [28, 30].

The rest of the parameters in Eq. (3) are $c = a\beta$, and $\overline{\eta} = (\sum_i \eta_i)/\sqrt{N}$, which denotes a new (population averaged) Gaussian noise with zero mean and delta function correlations. This population noise has the amplitude σ_v, which corresponds to a standard deviation of v when $h = 0$, and it is given by

$$\sigma_v = \frac{\beta\sigma_w}{\sqrt{N}}\tau_f^z\left(f_o^{z+1} + z\sigma_f^{z+1}\right). \tag{5}$$

Note that σ_v scales as $1/\sqrt{N}$, and it is a product of the intrinsic synaptic conductance noise and of the presynaptic neural activity. The latter implies that a higher presynaptic activity amplifies the current noise. Note also that fluctuations in the presynaptic firing rate ($\sim \sigma_f$) enter σ_v only when $z = 1$, which relates to the fact that these fluctuations are much faster ($\sim \tau_f$) than the internal variability in synapses ($\sim \tau_w$).

In Eq. (3), the postsynaptic firing rate r assumes its quasi-stationary value (due to time scale separation), and is related to v through (for details see the Methods):

$$r = \frac{1}{2}\left(-A^2\kappa + \sqrt{A^4\kappa^2 + 4A^2 v}\right), \tag{6}$$

where A is the postsynaptic firing rate amplitude, and κ is the intensity of firing rate

r adaptation. Broadly speaking, the magnitude of κ reflects the strength of neuronal self-inhibition due to adaptation to synaptic stimulation (see Eqs. 16 and 17 in the Methods). Generally, increasing κ leads to decreasing postsynaptic firing rate r (Fig. 1). For $\kappa = 0$, we recover a nonlinear firing rate curve (square root dependence on synaptic current v) that is characteristic for class one neurons [74, 75], while for sufficiently large κ, i.e. for $\kappa \gg 2\sqrt{v}/A$, we obtain a linear firing rate curve $r(v) \approx v/\kappa$ (Fig. 1A). Equations (3) and (6) form a closed system for determining the stochastic dynamics of the postsynaptic current v.

Bistability in mean-field synaptic current and an effective potential.

For cortical neurons the number of spines per neuron are very large ($N \sim 10^4$ [79, 80]), and thus one can expect that σ_v is small and consequently the fluctuations around the population average current v are rather weak. The results described below are obtained in the limit of very large N.

In the deterministic limit ($N \mapsto \infty$; $\sigma_v = 0$), the plasticity model in Eq. (3) can generate two stable stationary (steady-state) solutions corresponding to weak and strong currents/synapses. This can be seen by putting $dv/dt = 0$ in Eq. (3), and rearranging it to the form

$$v = g(v), \tag{7}$$

where the right hand side of this equation, $g(v) = \epsilon c f_o + \tau_w h r^2 (1 - \alpha r)$, and it depends

on v only through r as in Eq. (6). Moreover, the function $g(v)$ has a maximum with height proportional to h. When h is very small, Eq. (7) has only one solution $v \sim O(\epsilon)$ (i.e. one intersection point of the curves representing the functions on the right and on the left; Fig. 1B). This solution corresponds to weak synapses and monostable regime. Increasing h, by increasing f_0, causes an increase in the maximal value of the right hand side in Eq. (7), such that more solutions are possible (Fig. 1B). In particular, when h grows above a certain critical value h_{cr}, Eq. (7) generates 3 solutions (one $\sim O(\epsilon)$ and two other $\sim O(1)$), of which the middle one is unstable (Fig. 1B). This case corresponds to bistable regime with two stable solutions, representing weak and strong synaptic currents that can be called, respectively, "down" and "up" synaptic states. These two states could hypothetically be related to thin and mushroom dendritic spines, with small and large number of AMPA receptors, respectively [81]. For very large driving-plasticity h the two lower solutions disappear and we have again a monostable regime with strong synapses only (Fig. 1B).

A geometrical condition for the emergence of bistability is when the function $g(v)$ in Eq. (7) first touches tangentially the line $y = v$, i.e. when $dg/dv = 1$ (Fig. 1B). Solving this condition together with Eq. (6) yields for $\epsilon \ll 1$ the critical value of the driving-plasticity parameter h_{cr} as

$$h_{cr} = \frac{\alpha\kappa}{\tau_w}\left(1 + \sqrt{1 + (\alpha\kappa A^2)^{-1}}\right)^2 + O(\epsilon). \tag{8}$$

Note that for very fast decay in Eq. (3), i.e. for $\tau_w \mapsto 0$, the bistability is lost, since

then $h_{cr} \mapsto \infty$, and there is only one solution corresponding to weak synapses $v \sim O(\epsilon)$. Bistability is also lost in the opposite limit of extremely slow decay, $\tau_w \mapsto \infty$, but in this case the only solution corresponds to strong synapses. Interestingly, for very strong neural adaptation, $\kappa \mapsto \infty$, the bistability also disappears, since then $h_{cr} \mapsto \infty$. This case corresponds to extremely small postsynaptic firing rates, $r \approx v/\kappa \approx 0$ (Fig. 1A), and indicates the absence of a driving force capable of pushing synapses to a higher conducting state. On the other hand, when there is no adaptation, $\kappa \mapsto 0$, the critical $h_{cr} \mapsto (\tau_w A^2)^{-1}$, i.e. it is finite. This means that it is easier to produce synaptic bistability for neurons with stronger nonlinearity in their firing rate curves (see Eq. 6; Fig. 1A).

For N large but finite the description becomes probabilistic since $\sigma_v > 0$, and one can map Eq. (3) for the dynamics of v into an equation for the dynamics of the probability distribution of v conditioned on f_o, i.e. $P(v|f_o)$, described by a Fokker-Planck equation (see Eq. 26 in the Methods). In the stochastic stationary state, characterized by the stationary probability distribution $P_s(v|f_o)$, we can define a new and important quantity called an effective potential $\Phi(v|f_o)$, which is a function of the synaptic current v. The effective potential Φ is proportional to the amount of energy associated with the synaptic plasticity described by Eq. (3), and it is related to the stationary probability distribution $P_s(v|f_o)$ via $\Phi(v|f_o) \sim -\ln P_s(v|f_0)$ [58]. If we use a mechanical analogy and treat v as a spatial coordinate, then synaptic plasticity can be visualized as a movement in v space (state transitions), which is constrained by the energy related to Φ. This means that the shape of the function $\Phi(v)$ determines what

kind of motions in v-space (state space) are possible or more likely. In particular, the binary nature of synaptic plasticity given by Eq. (3) can be described as transitions between two wells of the effective potential $\Phi(v|f_0)$, corresponding to weak and strong synapses (e.g. [24, 32, 39]). These transitions can be thought as "hill climbing" process in the v space, which requires energy due to a barrier separating the two wells (Fig. 2).

The effective potential Φ can be found explicitly as (see the Methods)

$$\Phi(v|f_o) = \frac{v}{\tau_w}\left(\frac{1}{2}v - \epsilon c f_o\right) - h\left[\kappa r^3\left(\frac{1}{3} - \frac{\alpha r}{4}\right) + \frac{r^4}{A^2}\left(\frac{1}{2} - \frac{2\alpha r}{5}\right)\right]. \tag{9}$$

Note that the second term in Φ (with the large bracket) is proportional to the plasticity amplitude λ through h. This term depends on v through the firing rate r (see Eq. 6). In general, the functional form of the potential $\Phi(v|f_o)$ determines the thermodynamics of synaptic memory, and thus it is an important function.

The shape of the potential $\Phi(v|f_o)$ depends on the relative magnitude of the driving-plasticity h and the inverse of the decay time constant $1/\tau_w$ (Fig. 2A). In fact, there are two competing terms in Φ that are controlled by $1/\tau_w$ and h. The first term ($\sim 1/\tau_w$) maintains monostability, while the second ($\sim h$) promotes bistability. For h greater than the critical value h_{cr} (Eq. 8), there is bistability and Φ has two minima corresponding to up (strong) and down (weak) synaptic states (Fig. 2A), similar to the result for the deterministic limit. For very large h, there is again only one minimum related to strong synapses (Fig. 2A).

Due to fluctuations in the presynaptic input and in the internal synaptic machinery,

the mean-field synaptic current v can make occasional transitions between up and down states, which makes it effectively metastable. The dwelling times in both states (T_u, T_d) can be found from the classic Kramers "escape" formula (Eq. 29; [58]), and they are generally much larger than the time constant τ_w (Fig. 2B). The characteristic memory time T_m in the synaptic system is strictly related to T_u and T_d by Eq. (32). Generally, the memory lifetime is very small in the monostable regime ($T_m \sim \tau_w$), i.e. for small presynaptic firing (Fig. 2B). However, it jumps by several orders of magnitude when synapses become bistable (i.e. when $h \approx h_{cr}$), but then T_m monotonically decreases with increasing f_o (Fig. 2B).

The probabilities for synaptic currents in up and down states, p_u and p_d, are proportional to the dwelling times T_u and T_d via Eq. (30). These probabilities are important for determining analytically synaptic energy rate and Fisher information (see below).

Energy rate of synaptic plasticity.

The power dissipated by synaptic plasticity $\dot{E}$, or its metabolic rate, is proportional to the average temporal rate of the effective potential decrease, i.e. $-\langle d\Phi(v|f_0)/dt\rangle$, where $\langle ...\rangle$ denotes averaging with respect to the probability distribution $P(v|f_o)$. Since the potential $\Phi(v|f_0)$ depends on time only through v, after rearranging we get $\dot{E} \sim -\langle (dv/dt)(d\Phi/dv)\rangle$. Thermodynamically, this formula is equivalent to the entropy production rate associated with the stochastic process described by Eq. (3), and represented by the effective potential $\Phi(v|f_o)$ [57, 60, 61, 62, 63]. The synaptic plasticity energy rate $\dot{E}$ can be found analytically using $1/N$ expansion, and in the steady state takes the form (see Methods):

$$\dot{E} = \frac{E_o \sigma_v^2}{4\tau_w} \sum_{i=d,u} \frac{p_i}{(\Phi_i^{(2)})^2} \left[3(\Phi_i^{(3)})^2 + 2\Phi_i^{(2)} \Phi_i^{(4)} \right] + O(1/N^2), \tag{10}$$

where E_o is the characteristic energy scale for variability in spine conductance (it provides a link with an underlying molecular processes; see the Methods), and $\Phi_i^{(n)}$ denotes the n^{th} derivatives of the potential with respect to v at $v = v_i$, which can be easily found from Eq. (9). Note that in Eq. (10) the terms of the order $O(1)$ disappear, and the first nonzero contribution to $\dot{E}$ is of the order $O(1/N)$, since $\sigma_v \sim 1/\sqrt{N}$. Moreover, to have nonzero power in this order, the potential $\Phi(v)$ must contain at least a cubic nonlinearity.

Eq. (10) indicates that energy is needed for plasticity processes associated with the potential Φ "hill climbing", which is in analogy to the energy needed for a particle trapped in a potential well (of a certain shape) to escape. The energetics of such a "motion" in the v-space depends on the shape of the potential, which is mathematically accounted for by various higher-order derivatives of Φ. Thus, a fraction of synapses that were initially in the down state (p_d) can move up the potential gradient to the up state by overcoming a potential barrier, but this requires the energy that is proportional to σ_v^2 and to the derivatives of the potential. By analogy, a similar picture holds for synapses that were initially in the up state. The prefactor σ_v^2 in Eq. (10) indicates that the transitions up↔down, as well as local fluctuations near these states, cost energy that is proportional to the intrinsic thermodynamic noise in spines ($\sim \sigma_w$) and presynaptic activity (including its fluctuations $\sim f_o^{z+1} + z\sigma_f^{z+1}$). The important point is that if there

is no intrinsic spine noise ($\sigma_w = 0$), then there are no transitions between the up and down states in the steady state, and consequently there is no energy dissipation ($\sigma_v = 0$), regardless of the fast presynaptic input magnitude. In such a noiseless stationary state, the plasticity processes described by Eq. (3) are energetically costless, since there are no net forces that can change synaptic weight, or mathematically speaking, that can push synapses in the v-space. (This is not true under non-stationary conditions when there is some temporal variability in one or more parameters in Eq. 3, leading to dissipation, but the focus here is on the steady state). This situation resembles the so-called "fluctuation-dissipation" theorem known from statistical physics [57, 58, 59], where thermal fluctuations always cause energy loss. In our case, this fluctuation-dissipation relationship underlines a key role of thermodynamic fluctuations for the metabolic load of synaptic plasticity.

The synaptic energy rate (Eq. 10) depends on neurophysiological parameters that are hidden in the derivatives of Φ. The exact dependencies on these parameters are complicated, but we can make some approximations and obtain a more explicit formula for $\dot{E}$. The two basic approximations are that (i) the current v in the down state is small $O(\epsilon)$, and (ii) the coexistence of up and down states takes place mostly for h close to h_{cr} (transition point to bistability), such that the term $(h - h_{cr})^{-1}$ is relatively large. Taking these steps into account the approximate form of $\dot{E}$ is

$$\dot{E} \approx \frac{3E_o\sigma_v^2 h}{4[\kappa + O(\epsilon)]^4}\left(4p_d\left[h\tau_w + \alpha\kappa + \frac{2}{A^2}\right] + \frac{\alpha^2\kappa^2 B p_u}{\tau_w(h - h_{cr})}\right) + O(\epsilon), \tag{11}$$

where B is the dimensionless parameter $B = (1+\sqrt{1+d})^4/[\sqrt{1+d}(1+2d+\sqrt{1+d})^2]$, with $d = (\alpha\kappa A^2)^{-1}$ (B is between 0 and 4). The second term in the large bracket $\sim p_u$ is present only when $h > h_{cr}$, i.e. when there is synaptic bistability ($p_u > 0$).

Eq. (11) has an interesting interpretation. The terms in the large bracket proportional to p_d and p_u are proportional to the energy rates associated with the transitions down $\rightarrow$ up and up $\rightarrow$ down, respectively. These transitions cost energy because they are associated with overcoming the potential barrier separating the up and down states. Interestingly, the cost of the transition from the down to up state is proportional to $h\tau_w$, i.e. driving-plasticity parameter, and inversely proportional to the amplitude of postsynaptic firing rate $1/A^2$. The latter means that for large amplitude A, the transitions down $\rightarrow$ up are less likely and hence they cost less energy. The opposite is true for the transitions up $\rightarrow$ down (terms $\sim p_u$), which are enhanced for large A (through the parameter B), and hence cost more energy. Moreover, the transition up $\rightarrow$ down is amplified and is very energetic for h close to h_{cr}, i.e. in the regime when bistability first appears. This is due to the factor $(h - h_{cr})^{-1}$ present in Eq. (11), which signifies a sort of phase transition up$\leftrightarrow$down. For h larger than h_{cr}, the transitions from the up to down states are rare and consequently they use less energy; this is the regime of energetic efficiency (see also below). However, when $h \gg h_{cr}$, there is only the up state ($p_d \mapsto 0$; Fig. 2A) with large fluctuations around it that cost progressively more energy (the prefactor $\sigma_v^2 h$ grows with firing rate f_0 and with h).

The dependence of the synaptic plasticity metabolic rate on the average presynaptic firing f_o is shown in Fig. 3, together with a comparison of the exact and approximate

formulas for $\dot{E}$ (Eqs. 10 and 11). Generally, the energy rate $\dot{E}$ for $z = 1$ is about two-three orders of magnitude larger than for $z = 0$, which are the cases for synaptic noise either multiplied by presynaptic firing rate or not. For $z = 0$, the approximation to $\dot{E}$ given by Eq. (11) is very good only for low firing rate; at higher frequencies they start to deviate (Fig. 3). For $z = 1$, the approximation to $\dot{E}$ is very good in a broad range of f_o except at the transition point to bistability ($h \approx h_{cr}$). The behavior of $\dot{E}$ on f_o can be divided roughly into three phases, which are determined chiefly by whether synapses are in mono- or bistable regimes. In both cases of z, the energy rate $\dot{E}$ starts from a low level at monostable regime and increases weakly with increasing f_o up to an onset of bistability, where the behavior of $\dot{E}$ is dramatically different for $z = 0$ and $z = 1$ (Fig. 3). For $z = 1$ there is a sharp peak in the energy rate for $h \approx h_{cr}$ (phase transition) accompanied by a subsequent broad minimum (coexistence of weak and strong synapses), and then a monotonic increase of $\dot{E}$ for larger f_o (monostability with strong synapses). For $z = 0$ there is no peak at $h \approx h_{cr}$, but rather a cusp, and then there is a monotonic increase of $\dot{E}$ with increasing f_o. The lack of the peak for $z = 0$ is related to the fact that p_u increases weakly and smoothly form extremely small values without a sudden jump as for $z = 1$, which effectively smoothes out the behavior of $\dot{E}$ (see also below).

The results in Fig. 3 show that the cases with $z = 0$ and $z = 1$ differ qualitatively in terms of the dependence of p_d, p_u and $\dot{E}$ on the average presynaptic firing rate f_o. For $z = 0$, there are sharp transitions form synaptic monostability to bistability, and generally the bistable region is very narrow in comparison to the case for $z = 1$. This

implies that for $z = 0$, the synapses are mostly either exclusively in the down or in the up state, which does not seem to be realistic. For that reason, in the remaining of the paper, we focus mostly on the case with a broad bistable coexistence, i.e. the case $z = 1$.

Energy cost of plastic synapses as a fraction of neuronal energy cost: comparison to experimental data.

In order to assess the magnitude of the synaptic plasticity energy rate, we compare it to the rate of energy consumption by a typical cortical neuron for short-term signaling and maintaining of the resting potential [10]. The neural signaling includes spiking activity and synaptic transmission, which are known to consume the majority of the neural energy budget [10, 16, 17]. The ratio of the total energy rate used by plastic synapses $N\dot{E}$ to the neuron's energy rate $\dot{E}_n$ (given by Eq. (40)) is computed for different presynaptic firing rates and different cortical regions. In Figs. 4 and 5, we show the results for human and macaque cerebral cortex. These plots indicate that synaptic plasticity contribution depends strongly on the presynaptic firing rate f_o, and ranges from negligible ($\sim 0.001-0.01\%$) to substantial ($\sim 20-30\%$), depending mostly on the proximity to the point of bistable phase transition, cortical area, and neuronal firing rate adaptation κ (Figs. 4 and 5). For example, for human cortex the ratio $N\dot{E}/\dot{E}_n$ is generally larger in the visual cortex than in the frontal (Fig. 4), whereas for macaque cortex the reverse is observed (Fig. 5). Moreover, the plasticity contributions to neuronal metabolism are qualitatively very similar for human and macaque cortex, despite large differences in their sizes (compare Figs. 4 and 5).

Information encoded by plastic synapses.

Information or memory written in the synaptic structure about the average input f_o is encoded in the synaptic current probability distribution $P(v|f_0)$. This distribution is exponentially related to the potential $\Phi(v|f_0)$ in the stochastic steady state (see Eq. 27). Accuracy of the encoded information can be characterized by Fisher information I_F [82]. In general, larger I_F implies a higher coding precision. Fisher information can be derived analytically (see the Methods) as

$$I_F(f_o) = \frac{\tau_w^2 p_u p_d}{\sigma_v^4}\left[\Delta\Phi'_{ud} - 2\frac{\sigma'_v}{\sigma_v}\Delta\Phi_{ud}\right]^2 [1 + O(1/N)] + O(1), \tag{12}$$

where $\Delta\Phi_{ud} = \Phi(v_u) - \Phi(v_d)$, with the currents v_u, v_d in the up and down states (Eq. 28), and the prime denotes a derivative with respect to f_o. Note that, in the leading order, I_F depends on the derivatives of Φ with respect to f_o.

The first term in Eq. (12) $\sim 1/\sigma_v^4 \sim N^2$ corresponds to the contribution from the bistable regime, and it is much larger than the contribution denoted as $O(1)$ corresponding to the monostability. In the bistable interval, I_F should have a maximum when $p_u p_d$ is maximal, i.e. when $p_u \approx p_d \approx 0.5$. In the monostable regime, the first term disappears and I_F becomes of the order of $O(1)$, which is the primary reason why I_F (and coding accuracy) is several orders of magnitude smaller when synapses are monostable (see below).

Accuracy and lifetime of synaptically stored information vs plasticity energy rate.

How the long-term energy used by synapses relates to the accuracy and persistence of stored information? The above results indicate that $\dot{E}$ and I_F depend inversely on the synaptic noise σ_v, suggesting that its lowering should be beneficial since gain in information is accompanied by a decrease in synaptic energy rate.

A more complicated picture emerges if other parameters are varied, notably driving presynaptic input f_o (Fig. 6). At the onset of bistability, Fisher information I_F and memory lifetime T_m both increase dramatically with a corresponding sharp increase in energy rate $\dot{E}$, which implies that initial improvement in information accuracy and its retention cost a huge amount of energy, which is something one can expect from a physical point of view [1, 2, 3, 4, 5]. However, for higher f_o, when weak and strong synapses coexist there is a different trend. In this coexistence region when fractions of weak and strong synapses are roughly similar, Fisher information has a second broad maximum, memory lifetime weakly decreases, whereas the synaptic energy rate exhibits a very broad minimum (Fig. 6). Moreover, this minimal value of $\dot{E}$ is on the level of values in the monostable phase. This implies that an improvement in memory fidelity in the bistable region does not require an additional energy load. For even higher presynaptic input, when synapses tend to monostability with only the up state present, $\dot{E}$ increases monotonically due to broad fluctuations around this state, while I_F and T_m decrease, which in turn indicates an inefficiency of information storing in this region. These considerations can be visualized by comparing the ratios of $I_F/\dot{E}$ and $T_m/\dot{E}$ with

energy rate $\dot{E}$ as a function of f_o (Fig. 7). It is shown that $I_F/\dot{E}$ and $T_m/\dot{E}$ have maxima corresponding to minimal values of $\dot{E}$. This means that the biggest gains in synaptic information precision and lifetime per energy used are achieved for the bistable phase where the energy expenditure for plasticity is the smallest (Fig. 7). Taken together, these results suggest that storing of accurate information in synapses can be relatively cheap, and thus metabolically efficient, but only in a region with comparable fractions of weak and strong synapses.

The dependence of $\dot{E}$, I_F, and T_m on the basic neurophysiological parameters $(\lambda, \kappa, \tau_w)$ is shown in Figs. (8-10). Qualitatively, these relationships are nonlinear and similar to the dependence of $\dot{E}$, I_F, and T_m on presynaptic firing f_o, with peaks at the onsets of bistability. Note that $\dot{E}$ generally increases with the plasticity amplitude λ, except the interval of a narrow peak (Fig. 8), and decreases strongly with neural adaptation κ (Fig. 9). The latter dependence is expected based on Eq. (11), where the energy rate $\dot{E}$ contains the prefactor $\sim 1/\kappa^4$. Physically, this reflects the fact that increasing κ causes the decrease in the postsynaptic firing rate r, which leads to less dissipated energy. Interestingly, for $\tau_w \mapsto \infty$, i.e. for extremely slow synaptic processes, we obtain that $\dot{E} \mapsto 0$, which implies that in this case synaptic plasticity could in principle be reversible, without dissipation (Fig. 10). This is a hint that the late phases of synaptic plasticity, related to memory consolidation could be energetically relatively cheap.

Precision of coding memory is restricted by sensitivity of synaptic plasticity energy rate on the driving input.

The above results suggest that synaptic energy utilization does not limit directly the coding precision of a stimulus, because there is no a simple relationship between Fisher information and power dissipated by synapses. However, a careful inspection of the curves in Fig. 6 suggests that there might be a link between I_F and the derivative of $\dot{E}$ with respect to the driving input f_o. In fact, it can be shown that in the most interesting regime of synaptic bistability, to the leading order in $1/N$ expansion, we have either (see the Methods)

$$I_F(f_o) = \frac{(p_u')^2}{p_u p_d}\left[1 + O(1/N)\right], \tag{13}$$

or equivalently

$$I_F(f_o) = \frac{(\dot{E}'/\Delta\dot{E})^2}{p_u p_d}\left[1 + O(1/N)\right], \tag{14}$$

where the prime denotes derivative with respect to f_o, and $\Delta\dot{E}$ is the difference between energy used by strong and weak synapses. It is important to stress that simple formulas (13) and (14) have a general character, since they do not depend explicitly on the potential Φ, and thus they are independent of the plasticity type model. Eq. (13) shows that synaptic coding precision increases greatly for sharp transitions from mono- to bistability, since then $(p_u')^2$ is large. Additionally, Eq. (14) makes an explicit connection

between precision of synaptic information and nonequilibrium dissipation. Specifically, the latter formula implies that to attain a high fidelity of stored information, the energy used by synapses $\dot{E}$ does not have to be large, but instead it must change sufficiently quickly in response to changes in the presynaptic input.

We can also estimate a relative error e_f in synaptic coding of the average presynaptic firing f_o. This error is related to Fisher information by a Cramer-Rao inequality $e_f \geq (f_o\sqrt{I_F})^{-1}$ [82]. Using Eq. (14), in our case this relation implies

$$e_f \geq \frac{\sqrt{p_u p_d}}{f_o|\dot{E}'/\Delta\dot{E}|}. \tag{15}$$

The value of the product $p_u p_d$ is in the range from 0 to 1/4. In the worst case scenario for coding precision, i.e. for $p_u p_d = 1/4$, this implies that a 10% coding error ($e_f = 0.1$), corresponds to the relative sensitivity of the plasticity energy rate on presynaptic firing $f_0|\dot{E}'/\Delta\dot{E}| = 5$. Generally, the larger the latter value, the higher precision of synaptic coding. In our particular case, this high level of synaptic coding fidelity is achieved for the larger neural adaptation ($\kappa = 0.012$), which uses less synaptic energy (Figs. 6 and 7). This is yet another indication that precise coding does not have to involve more energy; in this case the reverse is observed (Fig. 6).

3. Discussion

General summary.

Neural computation is thought to be metabolically expensive [7, 8, 9, 10, 11, 13, 16], and it must be supported by cerebral blood flow and constrained by underlying microvasculature and neuroanatomy [83, 84]. It is shown here that an important aspect of this computation, namely long-term synaptic plasticity involved in learning and memory, constitutes only a small fraction of that overall energy cost, and precise memory storing can be relatively cheap. This conclusion agrees qualitatively with the results of a recent study on synaptic plasticity and memory storing in a class of cascade plasticity models supported by empirical estimates [50].

Specifically, in this study, the energy cost of long-term synaptic plasticity was determined and compared to the accuracy and lifetime of an information stored at excitatory synapses. The plasticity model used is an extension of BCM synaptic plasticity [21], and is similar to the one analyzed in Ref. [77], except the form of the postsynaptic firing rate and the noise term. The key formulas for the synaptic energy rate and Fisher information (Eqs. 10 and 12) were derived analytically for the stochastic stationary state applying (i) the timescale separation between neural and synaptic plasticity activities, (ii) dimensional reduction, and (iii) using $1/N$ expansion (small synaptic fluctuations on a population level), where N is the average number of excitatory synapses per neuron. The formulas in Eqs. (10) and (12) contain various derivatives of the effective potential Φ, which encodes the plasticity rules and which is proportional to the potential energy associated with plasticity events related to synaptic weight variability. In

this scenario, the synaptic plasticity corresponds to a driven stochastic motion of the population averaged postsynaptic current v in the space constrained by the potential Φ, in analogy to a ball moving on a rugged landscape with a ball coordinate corresponding to v. Because our potential can exhibit two minima separated by a potential barrier, the plasticity considered here can be viewed as a stochastic process of "hill climbing", or transitions between the two minima (the idea of "synaptic potential" was used also in Refs. [24, 32, 39]).

The energy rate of plastic synapses $\dot{E}$ (power dissipated by plasticity) is the energy used for climbing the potential shape in v-space, and it is proportional to the average temporal rate of decrease in the potential, $-\langle d\Phi/dt\rangle$, due to variability in v. In terms of thermodynamics, the plasticity energy rate $\dot{E}$ is equivalent to the entropy production rate, because synapses like all biological systems operate out of thermodynamic equilibrium with their environment and act as dissipative structures [57]. Dissipation requires a permanent influx of energy from the outside (provided by blood flow [83]) to maintain synaptic structure, which in our case is the distribution of synaptic weight or strength. A physical reason for the energy dissipation in synapses is their submicroscopic size promoting relatively large internal thermal fluctuations that tend to wipe out the pattern of synaptic weights. Thermodynamically speaking, this means reducing the synaptic order and thus increasing synaptic entropy. To preserve the order, this increased entropy has to be "pumped out", in the form of heat, by investing some energy in the process, which relates to ATP consumption.

The thermal synaptic noise can be additionally enhanced by presynaptic input vari-

ability, and both of these factors interact nonlinearly and drive synapses far from thermodynamic equilibrium to two metastable states, weak and strong, which allows binary memory storing at some metabolic cost. As a consequence of the nonlinear interactions, and jumping between weak and strong states, the plasticity energy rate and accuracy of information coding in synapses depend highly nonlinearly on all essential neurophysiological parameters, such as presynaptic input, plasticity amplitude, postsynaptic firing rate adaptation, and plasticity time constant (Figs. 8-10). Despite these complexities, a simple general relationship was found that links the accuracy of stored information with the sensitivity of synaptic energy rate on driving input and probabilities for finding synapses in up and down states (Eqs. 13 and 14). These relationships are general in the sense that they are independent of a specific plasticity model, because they are not directly dependent on the potential Φ (the plasticity type is fully specified in the potential Φ; see Eq. 9). In addition, Eq. (14) reveals that there is a thermodynamic constraint on the fidelity of long-term synaptic information, suggesting a link between nonequilibrium thermodynamics and synaptic memory.

The synaptic bistability considered here emerges on a population level, i.e. for the effective Eqs. (3) and (6). This means that majority synapses of a neuron participate in a coordinated switching between up and down states, due to fluctuations in the presynaptic firings and internal thermal noise. This mechanism is different from a mechanism found in Refs. [70, 71], where bistability was reported on a level of a single synapse. (However, from these papers it is difficult to judge how long the potentiation lasts in the absence of presynaptic stimulation). Our scenario for bistability is conceptually

closer to the model of synaptic bistability proposed by Zenke et al 2015 [85], which also emerges on a population level. Interestingly, both models, the one presented here and the one in [85], exhibit the so-called anti-Hebbian plasticity, in the sense that LTP (i.e. $\dot{v} > 0$) appears for low firing rates, instead of LTD as for classical BCM rule. However, in the present model the initial LTP window is very narrow, and appears for very small postsynaptic firing rates $r < (cf_0/\kappa)\epsilon \sim O(\epsilon)$. This feature is necessary for stable bistability, and does not contradict experimental results on BCM rule verification [86], showing LTD for low firing rates. The reason is that these experiments were performed for firing rates above 0.1 Hz, leaving uncertainty about LTP vs. LTD for very low activity levels (or very long times).

The cooperativity in synaptic bistable plasticity found here is to some extent similar to the data showing that neighboring dendritic spines interact and tend to cluster as either strong or weak synapses [87, 88]. These clusters can be as long as single dendritic segments, which is called "clustered plasticity hypothesis" [87, 88]. However, the difference is that in the present model there are no dendritic segments, and spatial dependence is averaged over, which leads effectively to one synaptic "cluster" either with up or down states.

Out of two models of synaptic noise, i.e. $z = 0$ and $z = 1$ in Eq. (1), it seems that the case $z = 1$ better describes neurophysiological data, since it generates a much broader bistability regime (Fig. 3A).

Coding of more accurate information in synapses need not require an extra cost.

The most striking result of this study is that storing memory about presynaptic firing rate f_o does not have to be metabolically expensive. Strictly speaking, the information encoded at synapses, i.e., its accuracy and lifetime, do not have to correlate positively with the energy used by synapses (Figs. 6 and 7). Such a correlation is only present at the onset of synaptic bistability, where a dramatic increase in information precision and lifetime is accompanied by a sharp and large increase in energy rate, but not further. In fact, near the broad peak of Fisher information, when the probabilities of having weak and strong synapses are approximately equal, the synaptic energy rate $\dot{E}$ exhibits a declining tendency and is close to its minimum that is comparable to values of $\dot{E}$ in the monostable phase (Fig. 6). This result suggests an energetic efficiency of stored memory in the bistable synaptic regime, i.e. relatively high information gain per energy used (Fig. 7).

An additional support for the energetic efficiency of synaptic information comes from the fact that energy used $\dot{E}$ and coding precision I_F depend the opposite way on synaptic noise σ_v (compare Eqs. (10) and (12)). Thus, reducing σ_v (e.g. by decreasing σ_w) will simultaneously increase the precision of synaptic information and decrease synaptic dissipation.

Taken together, these findings are compatible with a recent study [89] showing that abstract stochastic systems with memory, operating far from thermodynamic equilibrium, can be the most predictive about an environment if they use minimal energy.

Fundamental relationship between synaptic coding precision and sensitivity of dissipated energy on driving input.

Estimating an external variable is never perfect, and it is shown here that synaptic coding accuracy is not restricted by available energy rate, but it is instead limited by the derivative of the energy rate with respect to an average input. The fundamental relationship linking memory precision and synaptic metabolic sensitivity is present in Eq. (14), which is valid regardless of the specific plasticity mechanism, as long as synapses can exist in two metastable states. This binary synaptic nature is a key feature enabling a high fidelity of long-term synaptic information [70], despite ongoing neural activity, which is generally detrimental to information storing [41]. Specifically, for realistic neurophysiological parameters, it is found that the lower bound on the relative coding error in synapses can reach 0.1 (for higher neuronal adaptation), which again indicates a high precision of the stored information despite large fluctuations in presynaptic neural activities (large σ_f).

Thermodynamics of memory storing and bistability.

The general lack of high energetic demands for sustaining accurate synaptic memory may seem non-intuitive, given an intimate relation between energy and information known from classical physics [3]. For example, transmitting 1 bit of information through synapses is rather expensive and costs 10^4 ATP molecules [7], and a comparative number of glucose molecules [17], which energetically is much higher ($\sim 10^5 kT$) than a thermodynamic minimum set by the Landauer limit ($\sim 1kT$) [1]. Moreover, one might expect that larger spines with more storing capacity in their molecular structures should

also use more energy for maintaining these structures by synthesizing more proteins to balance their degradation [30, 31]. Additionally, there are classic and recent theoretical results that show dissipation-error tradeoff for biomolecular processes [60, 61, 90, 91, 92]. How can we understand our result in that light?

First, there is a difference between transmitting information and storing it, primarily in their time scales, and faster processes generally need more power (see also below). Second, it is good to keep in mind a distinction between potential energy (correlated with spine size, number of proteins, etc) and dissipated energy (correlated with driving frequency, thermal fluctuations, and turnover rates of various processes making a spine). In our case, the decrease in the dissipated energy with increasing presynaptic input in the bistable phase is associated with the appearance and deepening of the second minimum in the effective potential that traps synapses and counteracts their large fluctuations, which are always associated with energy dissipation [57]. One can also use a different, information related, reasoning.

It is known from thermodynamics that erasing an information can be more energy costly than storing information [1, 2], since the former process is irreversible and is always associated with energy dissipation, and the latter can in principle be performed very slowly (i.e. in equilibrium with the environment) without any heat released. In our system, the information is maximal for intermediate presynaptic input generating metastability with two synaptic states (Fig. 2). If we decrease the input below a certain critical value, or increase it above a certain high level, our system becomes monostable, which implies that it does not store much information (entropy is close to zero). Thus,

the transition from bistability to monostability is equivalent to erasing the information stored in synapses, which according to the Landauer principle [1, 4] should cost energy.

Third, the papers showing energy-error tradeoff in biomolecular systems [60, 61, 92, 91, 90] use fairly linear (or weakly nonlinear) models, while in our model the plasticity dynamics is highly nonlinear (see Eqs. 1 and 3). Additionally, we consider the prediction of an external variable (average input f_o), in contrast to some of the biomolecular models [91, 90], which dealt with estimating errors in an internal variable.

Cost of synaptic plasticity in relation to other neural costs.

The energy cost of synaptic plasticity is a new and an additional contribution to the overall neural energy budget considered before and associated with action potentials, short-term synaptic transmission, maintenance of negative resting potential, and nonsignaling factors [10, 93]. Those earlier studies provided important order of magnitude estimates based on ATP turnover rates, but they had mainly a phenomenological character and cannot be directly applied to nonlinear phenomena underlying synaptic plasticity. Contrary, the current approach and the complementary approach taken in [50] are based on "first principles" taken from non-equilibrium statistical physics and in combination with neural modeling can serve as a basis for future more sophisticated calculations of energy used in excitatory synapses, possibly with inclusion of some molecular detail (e.g. [30, 31, 45]).

The estimates performed here indicate that for human and macaque cortex the energy dissipated by synaptic plasticity, thought of as binary changes in the mean-field synaptic current, is strongly dependent on the presynaptic firing rate. Consequently,

the plastic energy rate contribution can account for a total neuronal energy rate at the level of $\sim 0.01 - 20\%$, which means that for some intervals it can be negligible, while for others it can be significant (Figs. 4 and 5). This strong dependence on presynaptic firing is consistent with a strong dependence of CaMKII autophosphorylation level on Ca^{2+} influx frequency to a dendritic spine [94], which should translate to a similar dependence of ATP consumption rate related to protein activation on presynaptic firing. Moreover, these results raise the possibility of observing or measuring the energetics of synaptic plasticity. The results presented here indicate that the energy rate of plasticity depends nonmonotonically on firing rate with a large peak near the transition to bistability (Figs. 3-6). In contrast, the neuronal energy rate related to short-term signaling depends monotonically on firing rate (see Eq. 38 and Refs. [8, 10, 17]). Thus metabolic peaks of plasticity, however small they are, should in principle be detectable if a local cortical circuit is driven by frequencies promoting the onset of synaptic bistability. It is hard to propose a specific imaging technique for detecting synaptic plasticity peaks, but nevertheless, it seems that techniques relying on spectroscopy, e.g., near-infrared spectroscopy with its high spatial and temporal resolution, could be of help.

Regardless of whether the energetics of synaptic plasticity is observable or not, it could have some functional implications. For example, it was reported that small regional decreases in glucose metabolic rate associated with age, and presumably with synaptic decline, lead to significant cognitive impairment associated with learning [95].

A relatively small contribution of plasticity to global cortical metabolism for some intervals is in large part due to relatively slow dynamics of spine conductance decay,

quantified by $\tau_w \sim 1$ hr [76, 77], which characterizes early phase of LTP and LTD ($\dot{E} \sim 1/\tau_w$ in Eq. 10). Late phases of LTP and LTD, during which memory is consolidated, are much slower and they are governed by timescales of the orders of days [40, 53]. Consequently, one can expect that these processes, as well as equally slow homeostatic synaptic scaling [96], should be energetically inexpensive. The energetics of these very slow processes were not included in the budget of the energy scale E_o (present in Eq. 10, and estimated in the Methods), since we were concerned only with the early phases of LTP and LTD, which are believed to be described by BCM model (both standard and extended). Nevertheless, for the sake of completeness, we can estimate the energy cost of the late LTP and LTD, as well as energy requirement of changing spine volume (also not included in the budget of E_o).

It is believed that protein synthesis, which is associated with l-LTP and l-LTD, underlines synaptic consolidation and scaling [45]. There are roughly 10^4 proteins in PSD including their copies [97], on average each with $\sim 400 - 500$ amino acids, which are bound by peptide bonds. These bonds require 4 ATP molecules to form [93], which is $4 \cdot 20kT$ of energy [98]. This means that chemical energy associated with PSD proteins is about $(3.2 - 4.0) \cdot 10^8 kT$, i.e. $(1.6 - 2.0) \cdot 10^7$ ATP molecules, or equivalently $(1.4 - 1.75) \cdot 10^{-12}$ J. Given that an average lifetime of PSD proteins is 3.7 days [99], we obtain the energy rate of protein turnover as $\sim (4.6 - 5.8) \cdot 10^{-18}$ W, or $52 - 65$ ATP/s per spine. For human cerebral cortex with a volume of 680 cm^3 [100] and average density of synapses $3 \cdot 10^{11}$ cm^{-3} [101], we have $2 \cdot 10^{14}$ synapses. This means that the global energy cost of protein turnover in spines of the human cortex is $(9.2 - 11.5) \cdot 10^{-4}$

W, or equivalently $(1-1.3)\cdot 10^{16}$ ATP/s, which is extremely small ($\sim 0.01\%$) as human cortex uses about 5.7 Watts of energy [8].

The changes in spine volume are related directly to the underlying dynamics of actin cytoskeleton [102, 103]. We can estimate the energy cost of spine size using a mechanistic argument. Dendritic spine grows due to pressure exerted on the dendrite membrane by actin molecules. The reported membrane tension is in the range $(10^{-4}-1)$ kT/nm^2 [104], with the upper bound being likely an overestimate, given that it is close to the so-called rapture tension ($1-2$ kT/nm^2), when the membrane breaks [104]. A more reasonable value of the membrane tension seems to be 0.02 kT/nm^2, as it was measured directly [105]. Taking this value, we get that to create a typical 1 μm^2 of stable spine requires $2\cdot 10^4 kT$ or 10^3 ATP molecules. Since the actin turnover rate in spine is 1/40 sec^{-1} [102], which is also the rate of spine volume dynamics, we obtain that the cost of maintaining spine size is 25 ATP/s. This value is comparable but two-fold smaller than the ATP rate used for PSD protein turnover per spine ($52-65$ ATP/s) given above.

How do the costs of protein turnover and spine mechanical stability relate to the energy cost of e-LTP and e-LTD calculated in this paper using the extended BCM model? From Fig. 6, we get that the latter type of synaptic plasticity uses energy in the range $(10^{-4}-10^{-1})E_o$ per second per spine, depending mainly on the neural adaptation amplitude κ. Since the energy scale $E_o = 2.3\cdot 10^4$ ATP (see the Methods), we obtain that the energy cost of the plasticity related to e-LTP and e-LTD is $2.3-2300$ ATP/s, i.e., it can be $50-100$ times larger than the contributions from protein turnover

and spine volume changes. This result strongly suggests that the calculations of the energetics of synaptic plasticity based on the extended BCM model provide a large portion (perhaps even the majority) of the total energy required for the induction and maintenance of synaptic plasticity.

4. METHODS

Neuron model.

We consider a sensory neuron with a nonlinear firing rate curve (so called class one, valid for most biophysical models) and with activity adaptation given by [74, 75]

$$\tau_r \frac{dr}{dt} = -r + \bar{A}\sqrt{I_{syn} - s} \tag{16}$$

$$\tau_a \frac{ds}{dt} = -s + \bar{\kappa} r \tag{17}$$

where r is the instantaneous neuron firing rate with mean amplitude $\bar{A}$, s is the adaptation current (or equivalently self-inhibition) with the intensity $\bar{\kappa}$, τ_r and τ_a are the time constants for variability in neural firing and adaptation, and I_{syn} is the total excitatory synaptic current to the neuron provided by N excitatory synapses, i.e., $I_{syn} \sim \sum_i f_i w_i$ (see Eq. 19 below). In order to ensure a saturation of the firing rate r for very large number of synapses N, and for s to be relevant in this limit, $\bar{A}$ and $\bar{\kappa}$ must scale as $\bar{A} = A/\sqrt{N}$ and $\bar{\kappa} = N\kappa$. In a mature brain N can fluctuate due to structural plasticity, but we assume in agreement with the data [80] that there is some well defined average value of N.

The neuron is driven by stochastic presynaptic firing rates f_i $(i = 1, ..., N)$ that depend on time according to

$$\frac{df_i}{dt} = -\frac{(f_i - f_o)}{\tau_f} + \frac{\sqrt{2}\sigma_f}{\sqrt{\tau_f}}\xi_i \tag{18}$$

where f_o is the mean firing rate, τ_f is the time constant of temporal changes in f_i, σ_f is the firing rate noise amplitude, and ξ_i is the Gaussian white noise with zero mean and Delta function correlations, i.e., $\langle \xi_i(t) \rangle_\xi = 0$ and $\langle \xi_i(t)\xi_j(t') \rangle_\xi = \delta_{ij}\delta(t-t')$ [58]. The prefactor $\sqrt{2/\tau_f}$ in front of the noise ξ_i comes from the desire to have the stationary standard deviation of f_i equal exactly to σ_f.

The synaptic current I_{syn} has two additive components related to AMPA and NMDA receptors, $I_{syn} = I_{ampa} + I_{nmda}$, with the receptor currents

$I_{ampa} = q q_{ampa} |V_r| \tau_{ampa} g_{ampa} \sum_{i=1}^{N} f_i M_i^{ampa}$,

and

$I_{nmda} = q q_{nmda} |V_r| \tau_{nmda} g_{nmda} \sum_{i=1}^{N} f_i M_i^{nmda}$,

where q is the probability of neurotransmitter release, V_r is resting membrane potential of the neuron, g_{ampa} and g_{nmda} are single channel conductances of AMPA and NMDA receptors, q_{ampa} and q_{nmda} are probabilities of their opening with characteristic times τ_{ampa} and τ_{nmda}. The symbols M_i^{ampa} and M_i^{nmda} denote AMPA and NMDA receptor numbers for spine i. Data indicate that during synaptic plasticity the most profound changes are in the number of AMPA receptors M^{ampa} and opening probability of NMDA q_{nmda} [18, 28, 106]. We define the excitatory synaptic weight w_i as a weighted average of AMPA and NMDA conductances, i.e.,

$w_i = (\tau_{nmda} q_{nmda} M_i^{nmda} g_{nmda} + \tau_{ampa} q_{ampa} M_i^{ampa} g_{ampa}) / (\tau_{nmda} + \tau_{ampa})$.

This enables us to write the synaptic current per spine, i.e. $v = I_{syn}/N$ (which is more convenient to use than I_{syn}), as

$$v = \frac{\beta}{N} \sum_{i=1}^{N} f_i w_i, \tag{19}$$

where $\beta = q|V_r|(\tau_{nmda} + \tau_{ampa})$. The current per spine v is the key dynamical variable in our dimensional reduction procedure and subsequent analysis (see below).

Separation of time scales and dimensional reduction.

The time scales related to neuronal firing rates and firing adaptation τ_f, τ_r and τ_a are much faster than the time scale τ_w associated with synaptic plasticity. Therefore, for long times of the order of τ_w, firing rate r and postsynaptic current adaptation s are in quasi-stationary state, i.e., $dr/dt \approx ds/dt \approx 0$. This implies a set of coupled algebraic equations:

$$\begin{aligned} r &= A\sqrt{v - s/N} \\ s &= N\kappa r, \end{aligned} \tag{20}$$

which yields a quadratic equation for r, i.e., $r^2 + A^2\kappa r - A^2 v = 0$. The solution for r, which depends on v, is given by Eq. (6).

The equation for f_i (Eq. 18) can also be solved using the known methods of linear stochastic differential equations [58], and the result is

$$f_i(t) = f_o + \frac{\sqrt{2}\sigma_f}{\sqrt{\tau_f}} \int_{-\infty}^{t} dx\, \xi(x) e^{-(t-x)/\tau_f}. \tag{21}$$

This equation indicates that presynaptic firing rates fluctuate around average value f_o with standard deviation $\sim \sigma_f$. The important point is that these fluctuations are fast, on the order of τ_f ($\sim 0.1 - 1$ sec), which is much faster than the timescale τ_w. For $\tau_f \mapsto 0$, the fluctuations disappear due to suppressing nature of the exponent under the integral.

Now we focus on the population averaged synaptic current v. Since v is proportional to weights w_i, and because r depends directly on v, it is possible to obtain a closed form dynamic equation for plasticity of v. Thus, instead of dealing with N dimensional dynamics of synaptic weights, we study a one dimensional dynamics of the average current v. This dimensional reduction is analogous to observing the motion of a center of mass of many particle system, which is easier than simultaneous observation of the motions of all particles. Such an approach is feasible for an analytical treatment where one can directly apply the methods of stochastic dynamical systems and thermodynamics [58].

The time derivative of v, given by Eq. (19), is denoted with dot and reads

$\dot{v} = (\beta/N) \sum_{i=1} (\dot{f}_i w_i + f_i \dot{w}_i) \approx (\beta/N) \sum_{i=1} f_i \dot{w}_i$,

where we used the fact that fluctuations in f_i are much faster than changes in weights w_i, and hence f_i are in stochastic quasi-stationary states ($\langle df_i/dt \rangle_\xi \approx 0$). Now, using Eq. (1) for $\dot{w}_i$ and quasi-stationarity of θ, we obtain the following equation for $\dot{v}$:

$$\dot{v} = \frac{\lambda\beta}{N} r^2(1-\alpha r)\sum_{i=1}^{N} f_i^2 - \frac{1}{\tau_w}\left(v - \frac{\epsilon c}{N}\sum_{i=1}^{N} f_i\right) + \frac{\sqrt{2}\beta\sigma_w\tau_f^z}{N\sqrt{\tau_w}}\sum_{i=1}^{N} f_i^{z+1}\eta_i, \tag{22}$$

where $c = a\beta$. The next step is to perform averaging over fast fluctuations in presynaptic rate f_i (averaging over noise ξ), by assuming that noise in the presynaptic input and intrinsic noise in spines are uncorrelated, i.e. $\langle \eta_i \xi_i \rangle_{\eta,\xi} = \langle \eta_i \rangle_\eta \langle \xi_i \rangle_\xi = 0$.

We need to find the following three averages: $\langle \sum_{i=1}^{N} f_i \rangle_\xi$, $\langle \sum_{i=1}^{N} f_i^2 \rangle_\xi$, and $\langle \sum_{i=1}^{N} f_i^{z+1}\eta_i \rangle_\xi$ (for $z = 0, 1$).

From Eq. (21) it follows that $\langle f_i \rangle_\xi = f_0$, and thus the first average is

$$\langle \sum_{i=1}^{N} f_i \rangle_\xi = N f_o. \tag{23}$$

For the second average we also use Eq. (21) and write

$\sum_{i=1}^{N} \langle f_i^2 \rangle_\xi = N f_o^2 + 2\sqrt{2}(f_o \sigma_f / \sqrt{\tau_f}) \sum_i \int_{-\infty}^{t} dx \, \langle \xi_i(x) \rangle_\xi \, e^{(x-t)/\tau_f}$

$+ (2\sigma_f^2/\tau_f) \sum_i \int_{-\infty}^{t} dx_1 \int_{-\infty}^{t} dx_2 \, \langle \xi_i(x_1)\xi_i(x_2) \rangle_\xi \, e^{(x_1+x_2-2t)/\tau_f}$.

Since $\langle \xi_i(x) \rangle_\xi = 0$ and $\langle \xi_i(x_1)\xi_i(x_2) \rangle_\xi = \delta(x_1 - x_2)$, we find the second average as

$$\langle \sum_{i=1}^{N} f_i^2 \rangle_\xi = N(f_o^2 + \sigma_f^2). \tag{24}$$

The third average can be decomposed as $\langle \sum_{i=1}^{N} f_i^{z+1}\eta_i \rangle_\xi = \sum_{i=1}^{N} \langle f_i^{z+1} \rangle_\xi \, \eta_i$, since the

noise η is independent of the noise ξ. For $z = 0$, we obtain directly from Eq. (21) that $\langle f_i \rangle_\xi = f_o$, while for $z = 1$ we have again $\langle f_i^2 \rangle_\xi = f_o^2 + \sigma_f^2$. Thus, the third average can be written as

$$\langle \sum_{i=1}^{N} f_i^{z+1} \eta_i \rangle_\xi = N(f_o^{z+1} + z\sigma_f^{z+1})\eta_i. \tag{25}$$

The final step is to insert the averages in Eqs. (23-25) into the equation for $\dot{v}$ (Eq. 22). As a result we obtain Eq. (3) in the main text, which is a starting point for determining energetics of synaptic plasticity and information characteristics.

Distribution of synaptic currents: weak and strong synapses.

Stochastic Eq. (3) for a population averaged synaptic current v corresponds to the following Fokker-Planck equation for the current probability distribution $P(v|f_o;t)$ conditioned on f_o [58]:

$$\frac{\partial P(v|f_o;t)}{\partial t} = -\frac{\partial}{\partial v}\left(F(v)P(v|f_o;t)\right) + \frac{\sigma_v^2}{\tau_w}\frac{\partial^2 P(v|f_o;t)}{\partial v^2}, \tag{26}$$

where the function $F(v) = hr^2(1 - \alpha r) - (v - \epsilon c f_o)/\tau_w$, with $h = \lambda\beta(f_o^2 + \sigma_f^2)$, and r depends on v as in Eq.(6). The stationary solution of this equation is of the form [58]

$$P_s(v|f_o) = Z(f_o)^{-1} \exp\left(-\frac{\tau_w}{\sigma_v^2}\Phi(v|f_o)\right), \tag{27}$$

where $Z(f_o)$ is the normalization factor dependent on f_o, and the effective potential $\Phi(v|f_o)$ for synaptic current v is $\Phi(v|f_o) = -\int_0^v dx\ F(x)$. The explicit form of $\Phi(v|f_o)$ is shown in Eq. (9).

Local minima of Φ correspond to metastable states, and their number is conditioned on whether the driving-plasticity parameter h is greater than the critical value h_{cr} given by Eq. (8). This critical value can be alternatively found by requiring that the second derivative of the potential Φ becomes positive in the up state. For $h < h_{cr}$, the potential Φ has one minimum related to weak currents or weak synapses (monostability), while for $h > h_{cr}$ an additional minimum appears (bistability) that is related to strong currents or synapses. The two minima are separated by a maximum corresponding to a potential barrier. Metastable values of v can be found from the condition $d\Phi/dv = 0$, which is equivalent to finding the fixed points of Eq. (3) in the deterministic limit. Formal solution of this nonlinear equation can be found using an ϵ expansion, i.e. $r = r_0 + r_1\epsilon + O(\epsilon^2)$, where $\epsilon \ll 1$ (see Suppl. Inform.). As a result of this procedure we obtain for down state (weak synapses) v_d and for up state v_u (strong synapses):

$$\begin{aligned} v_d &= c f_o \epsilon + O(\epsilon^2) \\ v_u &= \kappa r_u + (r_u/A)^2 + O(\epsilon) \end{aligned} \tag{28}$$

where $r_u = \left(h\tau_w - A^{-2} + \sqrt{(h\tau_w - A^{-2})^2 - 4\alpha\kappa h\tau_w}\right)/(2\alpha h\tau_w)$. The separating potential barrier between up and down states occurs for v_{max}, which has a similar form as v_u with the exception of a negative sign in front of the square root inside r_u.

Probabilities for weak and strong synapses.

In the bistable regime, the mean-field synaptic current can jump between up and down states. These transitions, depression and potentiation, are caused by fluctuations in the input firing rate f_i (proportional to σ_f) and internal thermodynamic fluctuations in synaptic conductance w_i (proportional to σ_w). From a physical point of view, this corresponds to a noise induced "escape" of some synapses through a potential barrier. Average dwelling times in the up (T_u) and down (T_d) states can be determined from the Kramers's formula [58]:

$$T_i = \frac{2\pi}{\sqrt{\Phi_i^{(2)}|\Phi_{max}^{(2)}|}} \exp\left(\frac{\tau_w}{\sigma_v^2}\Delta\Phi_i\right), \tag{29}$$

where the index $i = d$ or $i = u$, $\Phi_i^{(2)}$ and $\Phi_{max}^{(2)}$ are the second derivatives of the potential at its minima ($v = v_i$) and maximum ($v = v_{max}$), and the potential difference $\Delta\Phi_i = \Phi(v_{max}) - \Phi(v_i) > 0$. Note that for large number of synapses N, the exponential factor in Eqs. (29) can be large, which can lead to very long dwelling times that are generally much longer than any time scale in the original Eqs. (1-2) and (16-18). The

fact that the times T_u and T_d are long but finite is an indication of metastability of "locally" stable up and down synaptic states.

The probabilities for synapses in the up (p_u) and down (p_d) states can be determined using the above dwelling times as:

$$p_d = \frac{T_d}{T_d + T_u}, \tag{30}$$

and $p_u = 1 - p_d$. Note that when $T_u/T_d \ll 1$, most of the time synapses are in the lower state. Also, in the monostable regime where only down state is present, we set $p_u = 0$ by default.

Memory lifetime.

Synaptic memory lifetime T_m is defined as a characteristic time the synapses remember a perturbation to their steady state distribution. Mathematically, it means that we have to consider a time-dependent solution of the probability density $P(v|f_0;t)$ to the Fokker-Planck equation given by Eq. (26). This solution can be written as [58, 59]

$$P(v|f_o;t) = P_s(v|f_o) + \sum_{k=0}^{\infty} e^{-\gamma_k t}\psi_k(v|f_o), \tag{31}$$

where γ_k and $\psi_k(v|f_o)$ are appropriate eigenvalues and eigenvectors. The eigenvalues

are inverses of characteristic time scales, which describe a relaxation process to the steady state. The smallest eigenvalue, denoted as γ_0, determines the longest relaxation time $1/\gamma_0$, and we associate that time with the memory lifetime T_m. It has been shown that $\gamma_0 = 1/T_d + 1/T_u$ [58, 59], which implies that

$$T_m = \frac{T_u T_d}{T_u + T_d}. \tag{32}$$

A similar approach, through eigenvalues, to estimating the memory lifetime was adopted also in [107].

Approximation of the synaptic current distribution by bimodal distribution. In the limit of very large N the stationary distribution $P_s(v|f_o)$ has either one (monostability) or two (bistability) maxima corresponding to the minima of the potential $\Phi(v|f_o)$. For $N \mapsto \infty$ these maxima become sharp peaks, represented by delta functions at points v_d and v_u. This suggests that for large but finite N we can approximate $P_s(v|f_o)$ as a sum of two Gaussians centered at v_d and v_u that are weighted by the probabilities of synapses in the up and down states:

$$P_s(v|f_o) \approx P_s(v|f_o)_{app} = \sum_{i=d,u} \frac{p_i e^{-(v-v_i)^2/2\sigma_i^2}}{\sqrt{(\pi/2)\sigma_i^2}[1 + \mathrm{erf}(v_i/\sqrt{2\sigma_i^2})]} \tag{33}$$

where v is in the range $(0, \infty)$, $\mathrm{erf}(x)$ is the error function, and the effective standard

deviation σ_i of the synaptic current is given by $\sigma_i = \sigma_v/\sqrt{\tau_w \Phi_i^{(2)}} \sim 1/\sqrt{N}$, for up ($i = u$) and down ($i = d$) states, where $\Phi_i^{(2)}$ is the second derivative of the potential with respect to v at v_i. This approximation enables us to determine analytically the amount of dissipated energy by plastic synapses and accuracy with which they encode information.

Entropy production rate, entropy flux, and power dissipated by plasticity. Processes underlying synaptic plasticity are irreversible (e.g. AMPA receptor trafficking, PSD protein phosphorylation, as well as protein synthesis and degradation [28, 29]) and operate out of thermodynamic equilibrium, and therefore require energy influx. At a stochastic steady state, this energy is dissipated as heat, which roughly corresponds to a metabolic rate of synaptic plasticity. The rate of dissipated energy is proportional to the average rate of decrease in the effective potential Φ, or equivalently to the entropy production rate [57].

Given the above, we can write the energy rate for synaptic plasticity $\dot{E}$ as $\dot{E} \sim -\langle d\Phi(v|f_0)/dt\rangle = -\langle \Phi^{(1)}\dot{v}\rangle$, where $\Phi^{(1)}$ is the first derivative of Φ with respect to v, the symbol $\dot{v}$ is the temporal derivative of v, and the averaging $\langle ...\rangle$ is performed over the distribution $P(v|f_0)$. The second equality follows from the fact that v is the only variable in the potential that changes with time on the time scale τ_w. Next, we can use Eq. (3) in the equivalent form, namely $\dot{v} = -\Phi^{(1)} + \sqrt{2/\tau_w}\sigma_v\overline{\eta}$, and this equation resembles the motion of an overdamped particle (with negligible mass) in the potential Φ, with v playing the role of a spatial coordinate. After that step, we can write the

energy rate as $\dot{E} \sim \langle[\Phi^{(1)}]^2\rangle - \sqrt{2/\tau_w}\sigma_v\langle\Phi^{(1)}\overline{\eta}\rangle$. The final step is to use the Novikov theorem [108] for the second average, i.e. $\langle\Phi^{(1)}\overline{\eta}\rangle = \frac{1}{2}\sqrt{2/\tau_w}\sigma_v\langle\Phi^{(2)}\rangle$. This leads to $\dot{E} \sim \frac{\sigma_v^2}{\tau_w}\left(-\langle\Phi^{(2)}\rangle + (\tau_w/\sigma_v^2)\langle[\Phi^{(1)}]^2\rangle\right)$.

We can obtain a similar result for $\dot{E}$ using a thermodynamic reasoning. The dynamics of synaptic plasticity is characterized by the distribution of synaptic currents per synapse $P(v|f_o)$, which evolves in time according to Eq. (26). With this distribution we can associate the entropy $S(t)$, defined as $S(t) = -\int_0^\infty dv\ P(v|f_o)\ln P(v|f_o)$, measuring the level of order in a typical spine. It can be shown [57, 62, 63] that the temporal derivative of the entropy, dS/dt, is composed of two competing terms, $dS/dt = \Pi - \Gamma$, called entropy production rate (Π) and entropy flux (Γ), both per synapse. In the case of thermodynamic equilibrium, which is not biologically realistic, one has $dS/dt = \Pi = \Gamma = 0$, and there is neither energy influx to a system nor dissipated energy to the environment. However, for processes out of thermodynamic equilibrium, relevant for spine dynamics, we still can find a stationary regime where entropy of the spine does not change, $dS/dt = 0$, but entropy flux Γ and entropy production Π are nonzero and balance each other [57, 62]. It is more convenient to determine the stationary dissipated power by finding the entropy flux, which is given by [62, 63] (see Suppl. Infor.)

$$\Gamma = \frac{\tau_w}{\sigma_v^2}\langle[\Phi^{(1)}]^2\rangle - \langle\Phi^{(2)}\rangle \tag{34}$$

Note that Eq. (34) is very similar in form to the energy rate $\dot{E}$ derived above; the two expressions differ only by the factor σ_v^2/τ_w, and none of them has the units of energy (Γ

has the unit of the inverse of time). Thus, we need to introduce the energy scale in the problem. Generally, the stationary dissipated power per synapse $\dot{E}$ can be written as $\dot{E} = E_o\Pi = E_o\Gamma$ [57], where E_o is the characteristic energy scale associated with spine conductance changes, and its value is estimated in the next section.

It is not possible to find analytically the entropy flux Γ for an arbitrary probability distribution in Eq. (34). In particular, it is not feasible for the distribution $P_s(v|f_0)$ in Eq. (27). However, Γ can be explicitly determined for the approximation to $P_s(v|f_0)$ given by Eq. (33). Generally speaking, for very large synaptic number per neuron N, the probability distribution in Eq. (33) has two sharp maxima corresponding to two most likely synaptic currents v_d and v_u. Consequently, the values of v that are the closest to v_d and v_u provide the biggest contributions to the averages in the entropy flux Γ. The whole mathematical procedure is called a saddle point approximation, and it represents a series expansion in powers of $1/\sqrt{N}$ or the widths of the maxima σ_i, as both parameters are proportional. Specifically, for any differentiable function $G(v)$ with two peaks at $v = v_d$ and $v = v_u$, its average with respect to the approximate distribution $P_s(v|f_o)$ in Eq. (33) up to the order $1/N^2$ is (see Suppl. Info.):

$$\langle G(v)\rangle = \sum_{i=d,u} p_i \left(G_i + \frac{\sigma_i^2}{2} G_i^{(2)} + \frac{\sigma_i^4}{8} G_i^{(4)} \right) + O(\sigma_i^6), \tag{35}$$

where σ_i is given in Eq. (33), $G_i = G(v_i)$, and $G_i^{(2)}$, $G_i^{(4)}$ are the second and forth derivatives of G with respect to v at v_i. This equality enables us to find the averages $\langle[\Phi^{(1)}]^2\rangle$ and $\langle\Phi^{(2)}\rangle$ (see also Suppl. Info):

$$\langle \Phi^{(2)}(v) \rangle = \sum_{i=u,d} p_i \left[\Phi_i^{(2)} + (\sigma_i^2/2)\Phi_i^{(4)} \right] + O(\sigma_i^4), \tag{36}$$

where $\Phi_i^{(n)} = \Phi^{(n)}(v_i)$, and

$$\langle [\Phi^{(1)}(v)]^2 \rangle = \sum_{i=u,d} p_i \left(\sigma_i^2 (\Phi_i^{(2)})^2 + (\sigma_i^4/4)[3(\Phi_i^{(3)})^2 + 4\Phi_i^{(2)}\Phi_i^{(4)}] \right) + O(\sigma_i^6). \tag{37}$$

Note that $\Phi_i^{(1)} = -F(v_i) = 0$, which is the reason for the lack of the first derivative of Φ in Eq. (37). Having these averages, we can determine analytically the power per synapse $\dot{E}$. The result is Eq. (10) above.

Estimation of the characteristic energy scale for synaptic plasticity.

Dendritic spine is a composite object with multiple components and many degrees of freedom [25, 26, 27, 29], and hence the characteristic energy scale E_o is much bigger than kT, where k is the Boltzmann constant and T is the tissue absolute temperature ($T \approx 310$ K). The changes in spine conductance on time scale of ~ 1 hr, i.e. for e-LTP and e-LTD, are induced by protein interactions in PSD [30, 45] and subsequent membrane trafficking associated with AMPA and NMDA receptors [28, 29, 109]. Protein interactions are powered by phosphorylation process, which is one of the main biochemical mechanism of molecular signal transduction in PSD relevant for synaptic

plasticity [68, 110]. Phosphorylation rates in an active LTP phase can be very fast, e.g., for CaMKII autophosphorylation they are in the range $60 - 600$ min^{-1} [111]. Other processes in a spine, most notably protein turnovers in PSD (likely involved in l-LTP and l-LTD), are much slower ~ 3.7 days [99], and therefore their contribution to the energetics of the early phase of spine plasticity seems to be much less important (see, however Discussion for an estimate of the protein turnover energy rate).

The energy scale for protein interaction can be estimated as follows. A typical dendritic spine contains about 10^4 proteins (including their copies) [97]. One cycle of protein phosphorylation requires the hydrolysis of 1 ATP molecule [112, 113], which costs about $20kT$ [98]. Each protein has on average 4-6 phosphorylation sites [114, 115]. If we assume conservatively that only about 20% of all PSD proteins are phosphorylated, then we obtain the energy scale for protein interactions roughly $2 \cdot 10^5 kT$, which is $8.6 \cdot 10^{-16}$ J.

Energy scale for receptor trafficking can be broadly decomposed into two parts: energy required for insertion of the receptors into the spine membrane, and energy related to their horizontal movement along the membrane to the top near a presynaptic terminal. The insertion energy for a typical protein is either about $3-17$ kcal/mol [116] or $8 - 17kT$ [117], with the range spanning $4 - 25kT$, and is caused by a deformation in the membrane structure [116]. Since an average spine contains about 100 AMPA [118, 119] and 10 NMDA [120] receptors, we obtain the total insertion energy in the rage $500 - 3200kT$. The second, movement contribution can be estimated by noting that typical forces that overcome friction and push macromolecules along membrane

are about 10 pN, and they are powered by ATP hydrolysis [121]. AMPA and NMDA receptors have to travel a spine distance of about 1 μm [122], which requires the work of $110 \cdot 10^{-11} \cdot 10^{-6}$ N·m= $1.1 \cdot 10^{-15}$ J or $2.5 \cdot 10^5 kT$. The latter figure is 100 times larger than the insertion contribution, which indicates that the energy scale for receptor trafficking is dominated by the horizontal movement and is similar to the above for protein phosphorylation.

To summarize, the total energy scale E_o for spine conductance is about $E_o = 2 \cdot 10^{-15}$ J, or equivalently $4.6 \cdot 10^5 kT$ (or $2.3 \cdot 10^4$ ATP molecules).

Neuron energy rate related to short-term signaling.

We provide below an estimate of the energy used by a sensory neuron for short-term signaling for the sake of comparison with the energy requirement of synaptic plasticity. It has been suggested that the majority of neuronal energy goes to pumping out Na^+ ions (Na^+-K^+-ATPase), which accumulates mostly due to neural spiking activity, synaptic background activity, and passive Na^+ influx through sodium channels at rest [10]. It has been shown that this short-term neuronal energy cost can be derived from a biophysical neuronal model, compared across species, and represented by a relatively simple equation [8, 17]:

$$\mathrm{CMR}_{glu} = a_0 + a_1 \langle r \rangle + b \rho_s f_o, \tag{38}$$

where CMR_{glu} is the glucose metabolic rate [in μmol/(cm$^3\cdot$ min)], ρ_s is the synaptic density, $\langle r\rangle$ is the average postsynaptic firing rate, and the parameters a_0, a_1, and b characterize the magnitude of the above three contributions to the neural metabolism, i.e. resting, firing rate, and synaptic transmission, respectively [17]. The average postsynaptic rate $\langle r\rangle$ is found from Eq. (35):

$$\langle r\rangle = \sum_{i=u,d} p_i \left(r_i - \frac{\sigma_i^2 A^4}{(\kappa A^2 + 2r_i)^3} \right), \tag{39}$$

where $r_i = r(v_i)$ in Eq. (6).

According to biochemical estimates, one oxidized glucose molecule generates about 31 ATP molecules [123]. In addition, 1 ATP molecule provides about $20kT$ of energy [98]. This means that the short-term energy rate per neuron, denoted as $\dot{E}_n$, is given by

$$\dot{E}_n = 31 \cdot 20 \frac{N_A kT}{\rho_n} \mathrm{CMR}_{glu}, \tag{40}$$

where N_A is the Avogadro number, and ρ_n is the neuron density. We estimate the ratio of the synaptic plasticity power to neural power, i.e. $\dot{E}/\dot{E}_n$ across different presynaptic firing rates for three areas of the adult human cerebral cortex (frontal, temporal, and visual), and two areas of macaque monkey cerebral cortex (frontal and visual).

The values of the parameters a_0 and a_1 in Eq. (38) are species- and area-independent,

and they read $a_0 = 2.1 \cdot 10^{-10}$ mol/(cm^3 s), and $a_1 = 2.3 \cdot 10^{-9}$ mol/cm^3 [17]. The rest of the parameters take different values for human and macaque cortex. Most of them are taken from empirical studies, and are given below. The parameter b, present in Eq. (38), is proportional to the neurotransmitter release probability and synaptic conductance, and it was estimated based on fitting developmental data for glucose metabolism CMR$_{glu}$ and synaptic density ρ_s (which vary during the development) to the formula (38) [17].

The following data are for an adult human cortex. The adult CMR$_{glu}$ is 0.27 μmol/(cm^3·min) (frontal cortex), 0.27 μmol/(cm^3·min) (visual cortex), and 0.24 μmol/(cm^3·min) (temporal cortex) [124]. The parameter b reads: $1.16 \cdot 10^{-20}$ mol (frontal), $0.63 \cdot 10^{-20}$ mol (visual), $0.17 \cdot 10^{-20}$ mol (temporal) [17]. Note that the value of b is 7 times larger for the frontal cortex than for the temporal, which might suggest that the product of neurotransmitter release probability and synaptic conductance is also 7 fold larger in the frontal cortex. This high difference may seem unlikely, however, it is still plausible, given that the release probability is highly variable and can assume values between 0.05-0.7 [125, 126, 127, 128], and synaptic weights in the cortex are widely distributed [72]. Neuron density ρ_n reads: $36.7 \cdot 10^6$ cm^{-3} (frontal), $66.9 \cdot 10^6$ cm^{-3} (visual), $59.8 \cdot 10^6$ cm^{-3} (temporal) [129]. Synaptic density ρ_s reads: $3.4 \cdot 10^{11}$ cm^{-3} (frontal), $3.1 \cdot 10^{11}$ cm^{-3} (visual), $2.9 \cdot 10^{11}$ cm^{-3} (temporal) [101].

The following data are for an adult (6 years old) macaque monkey cortex. The adult CMR$_{glu}$ is 0.34 μmol/(cm^3·min) (frontal cortex), 0.40 μmol/(cm^3·min) (visual cortex) [130]. The parameter b reads: $0.4 \cdot 10^{-20}$ mol (frontal), and $3.8 \cdot 10^{-20}$ mol (visual) [17].

Neuron density ρ_n reads: $9 \cdot 10^7$ cm^{-3} (frontal), $31.9 \cdot 10^7$ cm^{-3} (visual) [131]. Synaptic density ρ_s reads: $5 \cdot 10^{11}$ cm^{-3} (frontal) [132], $6 \cdot 10^{11}$ cm^{-3} (visual) [133].

Fisher information and coding accuracy in synapses.

Fisher information $I_F(f_o)$ about the driving input f_o is a good approximation of the mutual information between the driving presynaptic activity and postsynaptic current v [134]. It is also a measure of the coding accuracy and it is defined as [82]

$$I_F(f_o) = \langle \left(\frac{\partial \ln P_s(v|f_o)}{\partial f_o} \right)^2 \rangle. \tag{41}$$

By a direct differentiation of Eq. (27) we get: $(\ln P_s)' = -(\ln Z)' - \tau_w(\Phi/\sigma_v^2)'$, where a prime denotes a derivative with respect to f_o. After averaging this expression, and noting that $\langle (\ln P_s)' \rangle = (\int_0^\infty dv P_s(v))' = 0$, we obtain $(\ln Z)' = -\tau_w \langle (\Phi/\sigma_v^2)' \rangle$. Thus, Fisher information reads:

$$I_F(f_o) = \tau_w^2 \left[\langle [(\Phi/\sigma_v^2)']^2 \rangle - \langle (\Phi/\sigma_v^2)' \rangle^2 \right]. \tag{42}$$

Applying Eq. (35) to $\langle [(\Phi/\sigma_v^2)']^2 \rangle$ and $\langle (\Phi/\sigma_v^2)' \rangle^2$, we obtain:

$$\langle \left[\left(\frac{\Phi}{\sigma_v^2} \right)' \right]^2 \rangle = \sum_{i=u,d} p_i \left(\left[\left(\frac{\Phi}{\sigma_v^2} \right)_i' \right]^2 + \sigma_i^2 \left(\frac{\Phi}{\sigma_v^2} \right)_i' \left(\frac{\Phi^{(2)}}{\sigma_v^2} \right)_i' \right) + O(\sigma_i^4), \tag{43}$$

and

$$\langle\left(\frac{\Phi}{\sigma_v^2}\right)'\rangle^2 = \left[\sum_{i=u,d} p_i \left(\frac{\Phi}{\sigma_v^2}\right)'_i\right]^2 + \left[\sum_{i=u,d} p_i \left(\frac{\Phi}{\sigma_v^2}\right)'_i\right]\left[\sum_{j=u,d} p_j \left(\frac{\Phi^{(2)}}{\sigma_v^2}\right)'_j \sigma_j^2\right] + O(\sigma_i^4). \quad (44)$$

Taking the difference of Eqs. (43) and (44), and noting that $p_i - p_i^2 = p_u p_d$, leads to Eq. (12) in the leading order.

Derivatives of dwelling times and of synaptic energy rate.

Below, we obtain the derivatives of the key quantities, with respect to f_0, in the bistable regime. The ratio of the dwelling times in up and down synaptic states T_u/T_d depends exponentially on N (through $1/\sigma_v^2$) and on the difference of potentials in these states (Eq. 29). Moreover, the potential Φ depends on input f_o. Thus, to the leading order in $1/N$ expansion, the biggest contribution to the derivative of T_u/T_d with respect to f_o (denoted with prime) provides the exponent in Eq. (29), i.e.

$$(T_u/T_d)' = -\frac{\tau_w}{\sigma_v^2}(T_u/T_d)\left[\Delta\Phi'_{ud} - 2\frac{\sigma_v'}{\sigma_v}\Delta\Phi_{ud}\right][1 + O(1/N)], \quad (45)$$

where $\Delta\Phi_{ud} = \Phi(v_u) - \Phi(v_d)$.

The energy rate given by Eq. (10) can be written equivalently as $\dot{E} = p_u\dot{E}_u + p_d\dot{E}_d$, where the energy rates for states near the up and down states are

$\dot{E}_i = \frac{E_o \sigma_v^2}{4\tau_w} \left[3(\Phi_i^{(3)})^2 + 2\Phi_i^{(2)} \Phi_i^{(4)} \right] / (\Phi_i^{(2)})^2,$

with $i = u, d$. Since the fractions p_u and p_d are proportional to the times T_u and T_d, and the latter are exponentially dependent on N, these fractions are the most sensitive parts in the energy rate $\dot{E}$ on changes in f_o to the leading order in $1/N$ expansion. Using Eqs. (30) and (45), we find derivatives of p_u and p_d with respect to f_o, and they take the forms

$$p_u' = -p_d' = -\frac{\tau_w p_u p_d}{\sigma_v^2} \left[\Delta\Phi_{ud}' - 2\frac{\sigma_v'}{\sigma_v} \Delta\Phi_{ud} \right] [1 + O(1/N)] \,. \tag{46}$$

Consequently, the f_o derivative of the energy rate is

$$\dot{E}' = -\frac{\tau_w p_u p_d}{\sigma_v^2} \Delta\dot{E} \left[\Delta\Phi_{ud}' - 2\frac{\sigma_v'}{\sigma_v} \Delta\Phi_{ud} \right] [1 + O(1/N)] \,, \tag{47}$$

where $\Delta\dot{E} = \dot{E}_u - \dot{E}_d$. If we combine Eqs. (12), (46) and (47), we obtain to the leading order Eqs. (13) and (14) in the Results for the bistable regime.

Parameters used in computations.

The following values of various parameters were used: $V_r = -65$ mV, $q = 0.35$ [127], $\tau_{nmda} = 150$ msec [120], $\tau_{ampa} = 5$ msec [119], $\tau_f = 1.0$ sec, $a = 1.0$ nS, $\alpha = 0.3$ sec [77], $\epsilon = 3 \cdot 10^{-4}$, $A = 600$ Hz$/\sqrt{nA}$, $\tau_w = 3600$ sec [76, 77], $\sigma_f = 10$ Hz [135], $\sigma_w = 1.0$ nS

[118, 119], $N = 1.6 \cdot 10^4$ [79, 80]. The two undetermined parameters are λ and κ, and two sets of values were used for them: $\kappa = 0.001$ (nA·sec), $\lambda = 9.36 \cdot 10^{-7}$ (nS·sec^2), and $\kappa = 0.012$ (nA·sec), $\lambda = 10.2 \cdot 10^{-6}$ (nS·sec^2), in order to obtain a transition to the bistable regime for $f_o \sim 1 - 5$ Hz. The value of A was chosen to obtain v_u in the neurophysiological range ~ 1 pA [71].

Supporting Information.

S1 Text. This file contains the details of some calculations. (PDF)

Acknowledgments

The work was supported by the Polish National Science Centre (NCN) grant no. 2015/17/B/NZ4/02600.

References

[1] Landauer R (1961) Irreversibility and heat generation in the computing process. *IBM J. Res. Dev.* **5**: 183-191.

[2] Bennett CH (1982) The thermodynamics of computation - a review. *Int. J. Theor. Physics* **21**: 905-940.

[3] Leff HS, Rex AF (1990) *Maxwell's Demon: Entropy, Information, Computing*. Princeton Univ. Press: Princeton, NJ.

[4] Berut A, Arakelyan A, Petrosyan A, Ciliberto S, Dillenschneider R, Lutz E (2012) Experimental verification of Landauer's principle linking information and thermodynamics. *Nature* **483**: 187-190.

[5] Parrondo JMR, Horowitz JM, Sagawa T (2015) Thermodynamics of information. *Nature Physics* **11**: 131-139.

[6] Levy WB, Baxter RA (1996) Energy efficient neural codes. *Neural Comput.* **8**: 531-543.

[7] Laughlin SB, de Ruyter van Steveninck RR, Anderson JC (1998) The metabolic cost of neural information. *Nature Neurosci.* **1**: 36-40.

[8] Karbowski J (2009) Thermodynamic constraints on neural dimensions, firing rates, brain temperature and size. *J. Comput. Neurosci.* **27**: 415-436.

[9] Aiello LC, Wheeler P (1995) The expensive-tissue hypothesis: The brain and the digestive-system in human and primate evolution. *Curr. Anthropology* **36**: 199-221.

[10] Attwell D, Laughlin SB (2001) An energy budget for signaling in the gray matter of the brain. *J. Cereb. Blood Flow Metabol.* **21**: 1133-1145.

[11] Karbowski J (2007) Global and regional brain metabolic scaling and its functional consequences. *BMC Biol.* **5**: 18.

[12] Balasubramanian V, Kimber D, Berry MJ (2001) Metabolically efficient information processing. *Neural. Comput.* **13**: 799-815.

[13] Niven B, Laughlin SB (2008) Energy limitation as a selective pressure on the evolution of sensory systems. *J. Exp. Biol.* **211**: 1792-1804.

[14] Logothetis NK (2008) What we can do and what we cannot do with fMRI. *Nature* **453**: 869-878.

[15] Alle H, Roth A, Geiger JRP (2009) Energy-efficient action potentials in hippocampal mossy fibers. *Science* **325**: 1405-1408.

[16] Harris JJ, Jolivet R, Attwell D (2012) Synaptic energy use and supply. *Neuron* **75**: 762-777.

[17] Karbowski J (2012) Approximate invariance of metabolic energy per synapse during development in mammalian brains. *PLoS ONE* **7**: e33425.

[18] Kasai H, Matsuzaki M, Noguchi J, Yasumatsu N, Nakahara H (2003) Structure-stability-function relationships of dendritic spines. *Trends Neurosci.* **26**: 360-368.

[19] Takeuchi T, Duszkiewicz AJ, Morris RGM (2014) The synaptic plasticity and memory hypothesis: encoding, storage and persistence. *Phil. Trans. R. Soc. B* **369**: 20130288.

[20] Markram H, Lubke J, Frotscher M, Sakmann B (1997) Regulation of synaptic efficacy by coincidence of postsynaptic APs and EPSPs. *Science* **275**: 213-215.

[21] Bienenstock EL, Cooper LN, Munro PW (1982) Theory for the development of neuron selectivity: orientation specificity and binocular interaction in visual cortex. *J. Neurosci.* **2**: 32-48.

[22] Miller KD, MacKay DJ (1994) The role of constraints in Hebbian learning. *Neural Comput.* **6**: 100-126.

[23] Song S, Miller KD, Abbott LF (2000) Competitive Hebbian learning through spike-timing-dependent synaptic plasticity. *Nat. Neurosci.* **3**: 919-926.

[24] van Rossum MCW, Bi GQ, Turrigiano GG (2000) Stable Hebbian learning from spike timing-dependent plasticity. *J. Neurosci.* **20**: 8812-8821.

[25] Bonhoeffer T, Yuste R (2002) Spine motility: phenomenology, mechanisms, and function. *Neuron* **35**: 1019-1027.

[26] Holtmaat AJ, Trachtenberg JT, Wilbrecht L, Shepherd GM, Zhang X, et al (2005) Transient and persistent dendritic spines in the neocortex in vivo. *Neuron* **45**: 279-291.

[27] Meyer D, Bonhoeffer T, Scheuss V (2014) Balance and stability of synaptic structures during synaptic plasticity. *Neuron* **82**: 430-443.

[28] Huganir RL, Nicoll RA (2013) AMPARs and synaptic plasticity: the last 25 years. *Neuron* **80**: 704-717.

[29] Choquet D, Triller A (2013) The dynamic synapse. *Neuron* **80**: 691-703.

[30] Lisman J, Yasuda R, Raghavachari S (2012) Mechanisms of CaMKII action in long-term potentiation. *Nat. Rev. Neurosci.* **13**: 169-182.

[31] Miller P, Zhabotinsky AM, Lisman JE, Wang X-J (2005) The stability of a stochastic CaMKII switch: Dependence on the number of enzyme molecules and protein turnover. *PLoS Biol.* **3**: e107.

[32] Billings G, van Rossum MC (2009) Memory retention and spike-timing-dependent plasticity. *J. Neurophysiol.* **101**: 2775-2788.

[33] Clopath C, Busing L, Vasilaki E, Gerstner W (2010) Connectivity reflects coding: a model of voltage-based STDP with homeostasis. *Nature Neurosci.* **13**: 344-352.

[34] Pfister JP, Gerstner W (2006) Triplets of spikes in a model of spike timing-dependent plasticity. *J. Neurosci.* **26**: 9673-9682.

[35] Tetzlaff C, Kolodziejski C, Timme M, Worgotter F (2011) Synaptic scaling in combination with many generic plasticity mechanisms stabilizes circuit connectivity. *Front. Comput. Neurosci.* **5**: 47.

[36] Toyoizumi T, Kaneko M, Stryker MP, Miller KD (2014) Modeling the dynamic interaction of Hebbian and homeostatic plasticity. *Neuron* **84**: 497-510.

[37] Costa RP, Froemke RC, Sjostrom PJ, Rossum MCW (2015) Unified pre- and postsynaptic long-term plasticity enables reliable and flexible learning. *eLife* **4**: e09457.

[38] Shouval HZ, Bear MF, Cooper LN (2002) A unified model of NMDA receptor-dependent bidirectional synaptic plasticity. *Proc. Natl. Acad. Sci. USA* **99**: 10831-10836.

[39] Graupner M, Brunel N (2012) Calcium-based plasticity model explains sensitivity of synaptic changes to spike pattern, rate, and dendritic location. *Proc. Natl. Acad. Sci. USA* **109**: 3991-3996.

[40] Ziegler L, Zenke F, Kastner DB, Gerstner W (2015) Synaptic consolidation: from synapses to behavioral modeling. *J. Neurosci.* **35**: 1319-1334.

[41] Fusi S, Drew PJ, Abbott LF (2005) Cascade models of synaptically stored memories. *Neuron* **45**: 599-611.

[42] Benna MK, Fusi S (2016) Computational principles of synaptic memory consolidation. *Nature Neurosci.* **19**: 1697-1706.

[43] Gutig R, Aharonov R, Rotter S, Sompolinsky H (2003) Learning input correlations through nonlinear temporally asymmetric Hebbian plasticity. *J. Neurosci.* **23**: 3697-3714.

[44] Smolen P, Baxter DA, Byrne JH (2012) Molecular constraints on synaptic tagging and maintenance of long-term potentiation: a predictive model. *PLoS Comput. Biol.* **8**: e1002620.

[45] Kandel ER, Dudai Y, Mayford MR (2014) The molecular and systems biology of memory. *Cell* **157**: 163-186.

[46] Chaudhuri R, Fiete I (2016) Computational principles of memory. *Nature Neurosci.* **19**: 394-403.

[47] Zenke F, Gerstner W (2017) Hebbian plasticity requires compensatory processes on multiple timescales. *Phil. Trans. R. Soc. B* **372**: 20160259.

[48] Engl E, Jolivet R, Hall CN, Attwell D (2017) Non-signalling energy use in the developing rat brain. *J. Cereb. Blood Flow Metab.* **37**: 951-966.

[49] Shulman RG, Rothman DL, Behar KL, Hyder F (2004) Energetic basis of brain activity: implications for neuroimaging. *Trends Neurosci.* **27**: 489-495.

[50] Karbowski J (2019) Metabolic constraints on synaptic learning and memory. *J. Neurophysiol.* **122**: 1473-1490.

[51] Cooper LN, Bear MF (2012) The BCM theory of synapse modification at 30: interaction of theory with experiment. *Nat. Rev. Neurosci.* **13**: 798-810.

[52] Izhikevich EM, Desai NS (2003) Relating STDP to BCM. *Neural Comput.* **15**: 1511-1523.

[53] Redondo RL, Morris RGM (2011) Making memories last: the synaptic tagging and capture hypothesis. *Nat. Rev. Neurosci.* **12**: 17-30.

[54] Lee SR, Escobedo-Lozoya Y, Szatmeri eM, Yasuda R (2009) Activation of CaMKII in single dendritic spines during long-term potentiation. *Nature* **458**: 299-304.

[55] Smolen P, Baxter DA, Byrne JH (2019) How can memories last for days, years, or a lifetime? Proposed mechanisms for maintaining synaptic potentiation and memory. *Learning and Memory* **26**: 133-150.

[56] Statman A, Kaufman M, Minerbi A, Ziv NE, Brenner N (2014) Synaptic size dynamics as an effective stochastic process. *PLoS Comput. Biol.* **10**: e1003846.

[57] Nicolis G, Prigogine I (1977) *Self-Organization in Nonequilibrium Systems*. Wiley: New York, NY.

[58] Van Kampen NG (2007) *Stochastic Processes in Physics and Chemistry*. Elsevier: Amsterdam.

[59] Risken H (1996) *The Fokker-Planck equation*. Springer: Berlin; pp. 121-132.

[60] Lan G, Sartori P, Neumann S, Sourjik V, Tu Y (2012) The energy-speed-accuracy trade-off in sensory adaptation. *Nature Physics* **8**: 422-428.

[61] Mehta P, Schwab DJ (2012) Energetic costs of cellular computation. *Proc. Natl. Acad. Sci. USA* **109**: 17978-17982.

[62] Tome T (2006) Entropy production in nonequilibrium systems described by a Fokker-Planck equation. *Braz. J. Physics* **36**: 1285-1289.

[63] Tome T, de Oliveira MJ (2010) Entropy production in irreversible systems described by a Fokker-Planck equation. *Phys. Rev. E* **82**: 021120.

[64] Seifert U (2012) Stochastic thermodynamics, fluctuation theoremes and molecular machines. *Rep. Prog. Phys.* **75**: 126001.

[65] Goldt S, Seifert U (2017) Stochastic thermodynamics of learning. *Phys. Rev. Lett.* **118**: 010601.

[66] Tkacik G, Mora T, Marre O, Amodei D, Palmer SE, Berry MJ, Bialek W (2015) Thermodynamics for a network of neurons: Signatures of criticality. *Proc. Natl. Acad. Sci. USA* **112**: 11508-11513.

[67] Friston K (2010) The free-energy principle: A unified brain theory? *Nat. Rev. Neurosci.* **11**: 127-138.

[68] Zhu J, Shang Y, Zhang M (2016) Mechanistic basis of MAGUK-organized complexes in synaptic development and signalling. *Nat. Rev. Neurosci.* **17**: 209-223.

[69] Montgomery JM, Madison DV (2004) Discrete synaptic states define a major mechanism of synaptic plasticity. *Trends Neurosci.* **27**: 744-750.

[70] Petersen CC, Malenka RC, Nicoll RA, Hopfield JJ (1998) All-or-none potentiation at CA3-CA1 synapses. *Proc. Natl. Acad. Sci. USA* **95**: 4732-4737.

[71] O'Connor DH, Wittenberg GM, Wang SSH (2005) Graded bidirectional synaptic plasticity is composed of switch-like unitary events. *Proc. Natl. Acad. Sci. USA* **102**: 9679-9684.

[72] Loewenstein Y, Kuras A, Rumpel S (2011) Multiplicative dynamics underlie the emergence of the log-normal distribution of spine sizes in the neocortex in vivo. *J. Neurosci.* **31**: 9481-9488.

[73] Bartol TM, Bromer C, Kinney J, Chirillo MA, Bourne JN, et al (2015) Nanoconnectomic upper bound on the variability of synaptic plasticity. *eLife* **4**: e10778.

[74] Ermentrout GB (1998) Linearization of F-I curves by adaptation. *Neural Comput.* **10**: 1721-1729.

[75] Ermentrout GB, Terman DH (2010) *Mathematical Foundations of Neuroscience*. Springer: New York, NY.

[76] Frey U, Morris RGM (1997) Synaptic tagging and long-term potentiation. *Nature* **385**: 533-536.

[77] Zenke F, Hennequin G, Gerstner W (2013) Synaptic plasticity in neural networks needs homeostasis with a fast rate detector. *PloS Comput. Biol.* **9**: e1003330.

[78] Jedlicka P, Benuskova L, Abraham WC (2015) A voltage-based STDP rule combined with fast BCM-like metaplasticity accounts for LTP and concurrent 'heterosynaptic' LTD in the dentate gyrus in vivo. *PloS Comput. Biol.* **11**: e1004588.

[79] Elston GN, Benavides-Piccione R, DeFelipe J (2001) The pyramidal cell in cognition: A comparative study in human and monkey. *J. Neurosci.* **21**: RC163 (1-5).

[80] DeFelipe J, Alonso-Nanclares L, Arellano JI (2002) Microstructure of the neocortex: Comparative aspects. *J. Neurocytol.* **31**: 299-316.

[81] Bourne J, Harris KM (2007) Do thin spines learn to be mushroom spines that remember? *Curr. Opin. Neurobiol.* **17**: 381-386.

[82] Cover TM, Thomas JA (2006) *Elements of Information Theory.* Wiley: Hoboken, NJ.

[83] Karbowski J (2014) Constancy and trade-offs in the neuroanatomical and metabolic design of the cerebral cortex. *Front. Neural Circuits* **8**: 9.

[84] Karbowski J (2015) Cortical composition hierarchy driven by spine proportion economical maximization or wire volume minimization. *PloS Comput. Biol.* **11**: e1004532.

[85] Zenke F, Agnes EJ, Gerstner W (2015) Diverse synaptic plasticity mechanisms orchestrated to form and retrieve memories in spiking neural networks. *Nat. Commun.* **6**: 6922.

[86] Kirkwood A, Rioult MG, Bear MF (1996) Experience-dependent modification of synaptic plasticity in visual cortex. *Nature* **381**: 526-528.

[87] Govindarajan A, Kelleher RJ, Tonegawa S (2006) A clustered plasticity model of long-term memory engrams. *Nat. Rev. Neurosci.* **7**: 575-583.

[88] Govindarajan A, Israely I, Huang SY, Tonegawa S (2011) The dendritic branch is the preferred integrative unit for protein synthesis-dependent LTP. *Neuron* **69**: 132-146.

[89] Still S, Sivak DA, Bell AJ, Crooks GE (2012) Thermodynamics of prediction. *Phys. Rev. Lett.* **109**: 120604.

[90] Barato AC, Seifert U (2015) Thermodynamic uncertainty relation for biomolecular processes. *Phys. Rev. Lett.* **114**: 158101.

[91] Bennett CH (1979) Dissipation-error tradeoff in proofreading. *BioSystems* **11**: 85-91.

[92] Lang AH, Fisher CK, Mora T, Mehta P (2014) Thermodynamics of statistical inference by cells. *Phys. Rev. Lett.* **113**: 148103.

[93] Engl E, Attwell D (2015) Non-signalling energy use in the brain. *J. Physiol.* **593**: 3417-3429.

[94] De Koninck P, Schulman H (1998) Sensitivity of CaM kinase II to the frequency of Ca^{2+} oscillations. *Science* **279**: 227-230.

[95] Gage FH, Kelly PAT, Bjorklund A (1984) Regional changes in brain glucose metabolism reflect cognitive impairments in aged rats. *J. Neurosci.* **4**: 2856-2865.

[96] Turrigiano GG, Nelson SB (2004) Homeostatic plasticity in the developing nervous system. *Nat. Rev. Neurosci.* **5**: 97-107.

[97] Sheng M, Hoogenraad CC (2007) The postsynaptic architecture of excitatory synapses: A more quantitative view. *Annu. Rev. Biochem.* **76**: 823-847.

[98] Phillips R, Kondev J, Theriot J, Garcia H (2012) *Physical Biology of the Cell*. Garland Science: London.

[99] Cohen LD, Zuchman R, Sorokina O, Muller A, Dieterich DC, Armstrong JD, et al. (2013) Metabolic turnover of synaptic proteins: kinetics, interdependencies and implications for synaptic maintenance. *PLoS ONE* **8**: e63191.

[100] Hofman MA (1988) Size and shape of the cerebral cortex in mammals. II. The cortical volume. *Brain Behav. Evol.* **32**: 17-26.

[101] Huttenlocher PR, Dabholkar AS (1997) Regional differences in synaptogenesis in human cerebral cortex. *J. Comparative Neurology* **387**: 167-178.

[102] Honkura N, Matsuzaki M, Noguchi J, Ellis-Davies GCR, Kasai H (2008) The subspine organization of actin fibers regulates the structure and plasticity of dendritic spines. *Neuron* **57**: 719-729.

[103] Cingolani L, Goda Y (2008) Actin in action: the interplay between the actin cytoskeleton and synaptic efficacy. *Nat. Rev. Neurosci.* **9**: 344-356.

[104] Phillips R, Ursell T, Wiggins P, Sens P (2009) Emerging roles for lipids in shaping membrane-protein function. *Nature* **459**: 379-385.

[105] Stachowiak JC, Brodsky FM, Miller EA (2013) A cost-benefit analysis of the physical mechanisms of membrane curvature. *Nature Cell Biol.* **15**: 1019-1027.

[106] Matsuzaki M, Honkura N, Ellis-Davies GCR, Kasai H (2004) Structural basis of long-term potentiation in single dendritic spines. *Nature* **429**: 761-766.

[107] Fusi S, Abbott LF (2007) Limits on the memory storage capacity of bounded synapses. *Nat. Neurosci.* **10**: 485-493.

[108] Novikov EA (1965) Functionals and the random-force method in turbulence theory. *Sov. Phys. JETP* **20**: 1290-1294.

[109] Borgdorff AJ, Choquet D (2002) Regulation of AMPA receptor lateral movements. *Nature* **417**: 649-653.

[110] Bhalla US, Iyengar R (1999) Emergent properties of networks of biological signaling pathways. *Science* **283**: 381-387.

[111] Bradshaw JM, Hudmon A, Schulman H (2002) Chemical quenched flow kinetic studies indicate an intraholoenzyme autophosphorylation

mechanism for Ca^{2+}/Calmodulin-dependent protein kinase II. *J. Biol. Chem.* **277**: 20991-20998.

[112] Hill TL (1989) *Free Energy Transduction and Biochemical Cycle Kinetics*. New York: Springer-Verlag.

[113] Qian H (2007) Phosphorylation energy hypothesis: Open chemical systems and their biological function. *Annu. Rev. Phys. Chem.* **58**: 113-142.

[114] Collins MO, Yu L, Coba MP, Husi H, Campuzano I, Blackstock WP, Choudhary JS, Grant SCN (2005) Proteomic analysis of in vivo phosphorylated synaptic proteins. *J. Biol. Chem.* **280**: 5972-5982.

[115] Trinidad JC, Barkan DT, Gulledge BF, Thaalhammer A, Sali A, Schoepfer R, Burlingame AL (2012) Global identification and characterization of both O-GlcNAcylation and phosphorylation at murine synapse. *Molecular & Cellular Proteomics* **11**: 215-229.

[116] Gumbart J, Chipot C, Schulten K (2011) Free-energy cost for translocon-assisted insertion of membrane proteins. *Proc. Natl. Acad. Sci. USA* **108**: 3596-3601.

[117] Grafmuller A, Shillcock J, Lipowsky R (2009) The fusion of membranes and vesicles: pathway and energy barriers from dissipative particle dynamics. *Biophys. J* **96**: 2658-2675.

[118] Matsuzaki M, Ellis-Davies GCR, Nemoto T, Miyashita Y, Iino M, Kasai H (2001) Dendritic spine geometry is critical for AMPA receptor expression in hippocampal CA1 pyramidal neurons. *Nat. Neurosci.* **4**: 1086-1092.

[119] Smith MA, Ellis-Davies GCR, Magee J (2003) Mechanism of the distance-dependent scaling of Schaffer collateral synapses in rat CA1 pyramidal neurons. *J. Physiol.* **548**: 245-258.

[120] Nimchinsky EA, Yasuda R, Oertner TG, Svoboda K (2004) The number of glutamate receptors opened by synaptic stimulation in single hippocampal spines. *J. Neurosci.* **24**: 2054-2064.

[121] Fisher ME, Kolomeisky AB (1999) Molecular motors and the forces they exert. *Physica* **A 274**: 241-266.

[122] Benavides-Piccione R, Fernaud-Espinosa I, Robles V, Yuste R, DeFelipe J (2013) Age-based comparison of human dendritic spine structure using complete three-dimensional reconstructions. *Cerebral Cortex* **23**: 1798-1810.

[123] Rolfe DFS, Brown GC (1997) Cellular energy utilization and molecular origin of standard metabolic rate in mammals. *Physiol. Revs.* **77**: 731-758.

[124] Chugani HT (1998) A critical period of brain development: Studies of cerebral glucose utilization with PET. *Preventive Medicine* **27**: 184-188.

[125] Bolshakov VY, Siegelbaum SA (1995) Regulation of hippocampal transmitter release during development and long-term potentiation. *Science* **269**: 1730-1734.

[126] Frick A, Feldmeyer D, Sakmann B (2007) Postnatal development of synaptic transmission in local networks of L5A pyramidal neurons in rat somatosensory cortex. *J. Physiol.* **585**: 103-116.

[127] Volgushev M, Kudryashov I, Chistiakova M, Mukovski M, Niesman J, et al (2004) Probability of transmitter release at neocortical synapses at different temperatures. *J. Neurophysiol.* **92**: 212-220.

[128] Murthy VN, Schikorski T, Stevens CF, Zhu Y (2001) Inactivity produces increases in neurotransmitter release and synapse size. *Neuron* **32**: 673-682.

[129] Pakkenberg B, Gundersen HJG (1997) Neocortical neuron number in humans: Effects of sex and age. *J. Comparative Neurology* **384**: 312-320.

[130] Noda A, Ohba H, Kakiuchi T, Futatsubashi M, Tsukada H, et al (2002) Age-related changes in cerebral blood flow and glucose metabolism in conscious rhesus monkeys. *Brain Res.* **936**: 76-81.

[131] Christensen JR, Larsen KB, Lisanby SH, Scalia J, Arango V, et al (2007) Neocortical and hippocampal neuron and glial cell numbers in the rhesus monkey. *Anatomical Record* **290**: 330-340.

[132] Bourgeois JP, Goldman-Rakic, PS Rakic P (1994) Synaptogenesis in the prefrontal cortex of rhesus monkeys. *Cereb. Cortex* **4**: 78-96.

[133] Bourgeois JP, Rakic P (1993) Changes of synaptic density in the primary visual cortex of the macaque monkey from fetal to adult stage. *J. Neurosci.* **13**: 2801-2820.

[134] Brunel N, Nadal JP (1998) Mutual information, Fisher information and population coding. *Neural Comput.* **10**: 1731-1757.

[135] Buzsaki G, Mizuseki K (2014) The log-dynamic brain: how skewed distributions affect network operations. *Nat. Rev. Neurosci.* **15**: 264-278.

Figure Captions

Fig. 1

Firing rates and emergence of bistability. (A) Postsynaptic firing rates r as functions of the population averaged synaptic current v for different neuronal adaptations values κ (in nA·sec). Increasing κ causes decrease in r and makes the functional form $r(v)$ more linear. (B) Graphical solutions of Eq. (7) and multiple roots for stationary v. For small driving-plasticity h there is only one intersection of $g(v)$ and the line $y = v$ at $v \sim O(\epsilon)$, corresponding to v_d and monostability (dashed red line; $f_0 = 0.3$ Hz, $\sigma_f = 8$ Hz). For higer h ($h > h_{cr}$) there are three intersections, but the middle one corresponds to an unstable solution, which in effect yields two stable solutions, i.e. bistability (dashed-dotted yellow line; $f_0 = 5.0$ Hz, $\sigma_f = 10$ Hz). When h is very large, then there is only one intersection, and it occurs for large v, corresponding to monostability with strong synapses v_u only (dotted green line; $f_0 = 15.0$ Hz, $\sigma_f = 10$ Hz). For both panels $z = 1$. Additionally, in panel (B), $\kappa = 0.001$ nA·sec, $\lambda = 9.36 \cdot 10^{-7}$ nS·sec^2.

Fig. 2

Effective synaptic potential, metastability, and memory lifetime. (A) The metastable synaptic states can be described in probabilistic terms and correspond to minima of an effective potential $\Phi(v|f_o)$. For weak presynaptic driving input f_o the potential Φ has only one minimum at $v_d \sim O(\epsilon)$, related to weak synapses. If f_o is above a certain threshold, then the potential displays two minima, corresponding to bistable coexistence of weak and strong synapses (v_d and v_u). In the bistable regime,

the synapses can jump between weak and strong states due to fluctuations in the input and/or synaptic noise. (B) Characteristic long times in the up (T_u), down (T_d) synaptic states, and memory lifetime T_m as functions of presynaptic firing f_o. Curves in (A) and (B) are for $z = 1$, and $\kappa = 0.001$ nA·sec, $\lambda = 9.36 \cdot 10^{-7}$ nS·sec^2; the rest of parameters as in the Methods.

Fig. 3.

Fraction of weak synapses and synaptic energy rate vs presynaptic firing: comparison of exact and approximate formulae. (A) Dependence of p_d on presynaptic firing rate f_o for $z = 0$ and $z = 1$. Note that for $z = 0$ the region of bistable coexistence is very narrow, i.e. p_d falls sharply from unity to zero. (B) Synaptic plasticity energy rate $\dot{E}$ as a function of f_o for $z = 0$ and $z = 1$. For $z = 0$, the approximate formula (dotted line; Eq. 11) gives a good match to the exact formula (solid line; Eq. 10) only for low firing rates f_o, whereas for $z = 1$ the approximate formula (dotted line) gives a good match to the exact formula (solid line) for a wide range of f_o, although the approximation overshoots for h close to h_{cr}. Note a pronounced peak for $z = 1$ when synapses become bistable, which is absent for $z = 0$.

Fig. 4.

Energy cost of synaptic plasticity as a fraction of neuron's energy cost for human cerebral cortex. The ratio of the total energy rate used by plastic synapses $N\dot{E}$ to neuron's energy rate $\dot{E}_n$ as a function of presynaptic firing rate f_o for different regions of the human cortex. Solid blue line corresponds to the visual cortex, dashed red line to the frontal cortex, and dotted green line to the temporal cortex. Note that

the ratio is the largest for the temporal cortex, and the smallest for the frontal cortex, and they can differ by an order of magnitude. This result has to do with the value of the empirically determined parameter b (proportional to synaptic weights and probability of neurotransmitter release) in Eq. (38) for neuronal CMR_{glu}, which is about 10 times larger for the frontal cortex than for the temporal (the ratio is inversely proportional to CMR_{glu}). For stronger neuronal adaptation κ (lower panel), the ratio is about two orders of magnitude smaller. Note that the energy contribution of plastic synapses to the neuron's energy budget is strongly dependent on f_o, and it could be substantial near the transition point to bistability. For all plots $z = 1$.

Fig. 5.

The same as in Fig. 4, but for macaque monkey cerebral cortex. Solid blue line corresponds to the macaque visual cortex, and dashed red line to the frontal cortex. The functional dependence for macaque cortex looks similar to the dependence for human cortex, except that the ratio is now larger for the frontal cortex. For all plots $z = 1$.

Fig. 6.

Comparison of synaptic energy rate with accuracy and lifetime of stored information as a function of presynaptic firing rate for $z = 1$**.** Note that at the onset of bistability $\dot{E}$, I_F, and T_m all have large peaks. In addition, I_F exhibit a second broad maximum in the bistable regime where the energy rate $\dot{E}$ is minimal. For solid lines $\kappa = 0.001$ nA·sec, and $\lambda = 9.36 \cdot 10^{-7}$ nS·sec^2, while for dotted line $\kappa = 0.012$ nA·sec, and $\lambda = 10.2 \cdot 10^{-6}$ nS·sec^2.

Fig. 7.

Gains in information accuracy and lifetime per synaptic energy used. The ratio $I_F/\dot{E}$ (upper panel) and $T_m/\dot{E}$ (middle panel) are compared to the synaptic energy rate $\dot{E}$ (lower panel) across different presynaptic firings. Note that $I_F/\dot{E}$ and $T_m/\dot{E}$ exhibit maxima in those locations where $\dot{E}$ has a broad minimum. For all panels $z = 1$. Parameters for solid and dotted lines as in Fig. 6.

Fig. 8.

Synaptic energy rate, Fisher information, and memory lifetime as functions of the plasticity amplitude λ. Note pronounced peaks at the onset of bistability. For all panels $z = 1$.

Fig. 9.

Synaptic energy rate, Fisher information, and memory lifetime as functions of firing rate adaptation κ. The general tendency is such that $\dot{E}$ decreases with κ, while I_F and T_m both increase (for small κ; bistable regime). Note pronounced peaks at the onset of bistability. For all panels $z = 1$.

Fig. 10.

Synaptic energy rate, Fisher information, and memory lifetime as functions of plasticity time constant τ_w. Note pronounced peaks at the onset of bistability. For all panels $z = 1$.

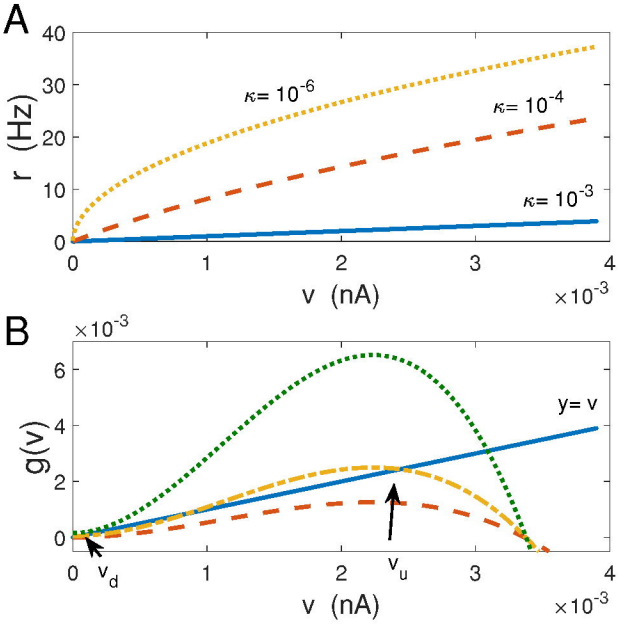
A
40
30
20
10
0
r (Hz)
κ= 10^{-6}
κ= 10^{-4}
κ= 10^{-3}
0
1
2
3
4
v (nA)
$\times 10^{-3}$
B
$\times 10^{-3}$
6
4
2
0
g(v)
y= v
0
v_d
1
2
v_u
3
4
v (nA)
$\times 10^{-3}$

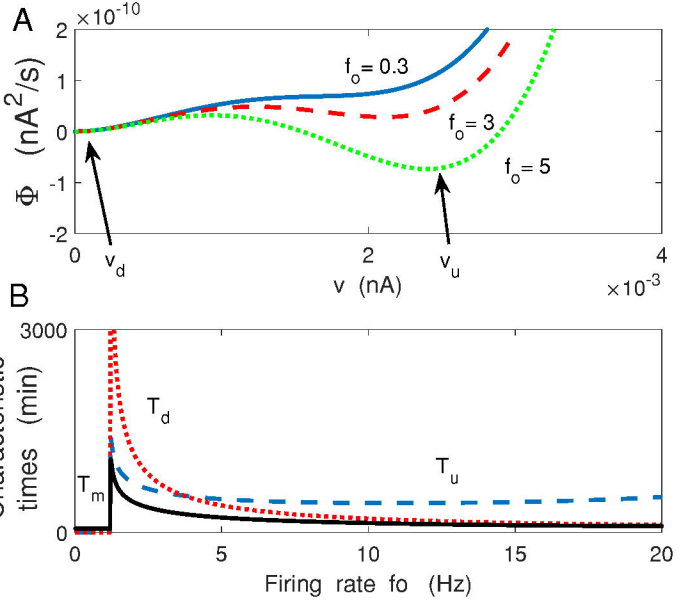
A
×10^-10
2
1
0
-1
-2
Φ (nA^2/s)
f_o= 0.3
f_o= 3
f_o= 5
0
v_d
2
v_u
4
v (nA)
×10^-3
B
3000
0
Characteristic times (min)
T_d
T_m
T_u
0
5
10
15
20
Firing rate fo (Hz)

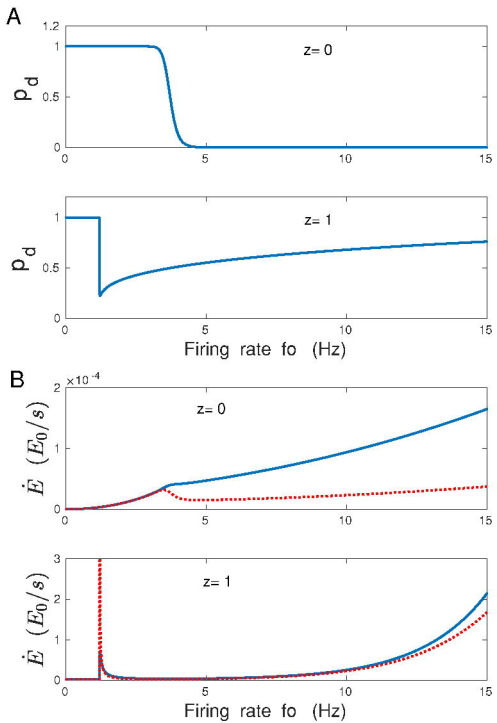
A
1.2
1
0.5
0
p_d
z= 0
0
5
10
15
1
0.5
0
p_d
z= 1
0
5
10
15
Firing rate fo (Hz)
B
$\times 10^{-4}$
2
1
0
$\dot{E}$ (E_0/s)
z= 0
0
5
10
15
3
2
1
0
$\dot{E}$ (E_0/s)
z= 1
0
5
10
15
Firing rate fo (Hz)

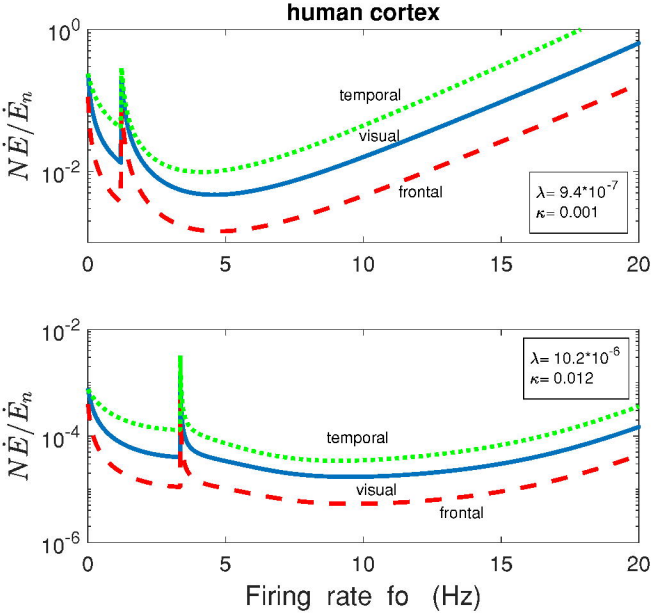
human cortex
10^0
10^{-2}
$N\dot{E}/\dot{E}_n$
temporal
visual
frontal
λ= 9.4*10^{-7}
κ= 0.001
0
5
10
15
20
10^{-2}
10^{-4}
10^{-6}
$N\dot{E}/\dot{E}_n$
λ= 10.2*10^{-6}
κ= 0.012
temporal
visual
frontal
0
5
10
15
20
Firing rate fo (Hz)

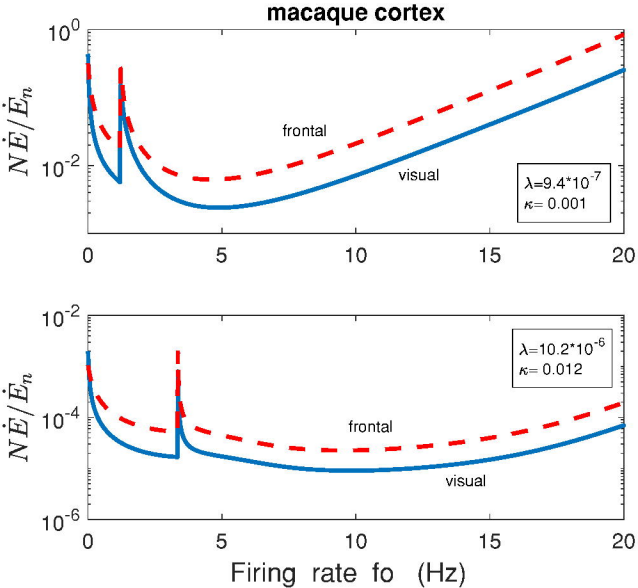
macaque cortex
10^0
10^{-2}
$N\dot{E}/\dot{E}_n$
frontal
visual
λ=9.4*10^-7
κ= 0.001
0
5
10
15
20
10^{-2}
10^{-4}
10^{-6}
$N\dot{E}/\dot{E}_n$
λ=10.2*10^-6
κ= 0.012
frontal
visual
0
5
10
15
20
Firing rate fo (Hz)

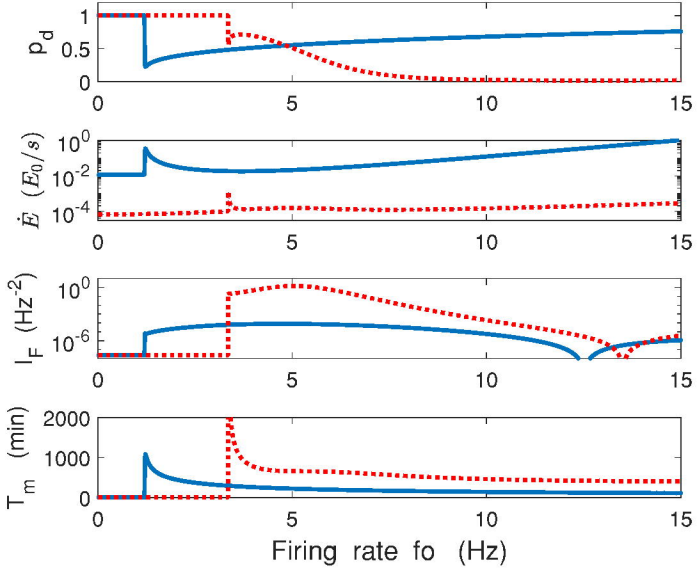
p_d
1
0.5
0
0
5
10
15
$\dot{E}$ (E_0/s)
10^0
10^{-2}
10^{-4}
I_F (Hz^-2)
10^0
10^{-6}
T_m (min)
2000
1000
0
Firing rate fo (Hz)

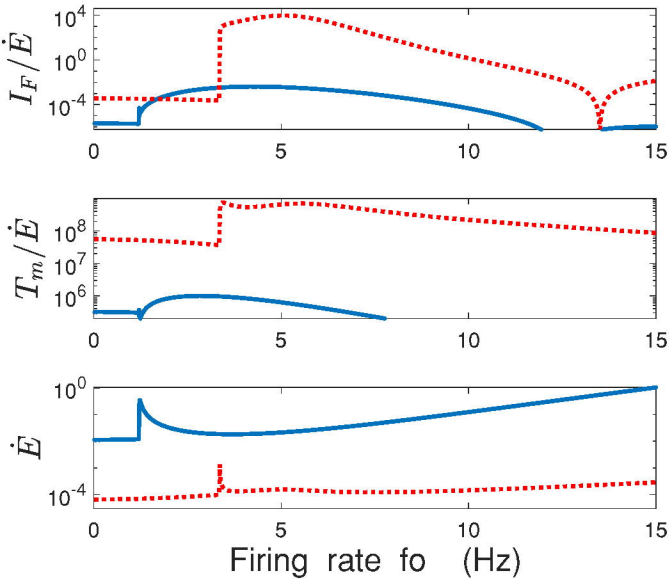
$I_F/\dot{E}$
10^4
10^0
10^{-4}
0
5
10
15
$T_m/\dot{E}$
10^8
10^7
10^6
0
5
10
15
$\dot{E}$
10^0
10^{-4}
0
5
10
15
Firing rate fo (Hz)

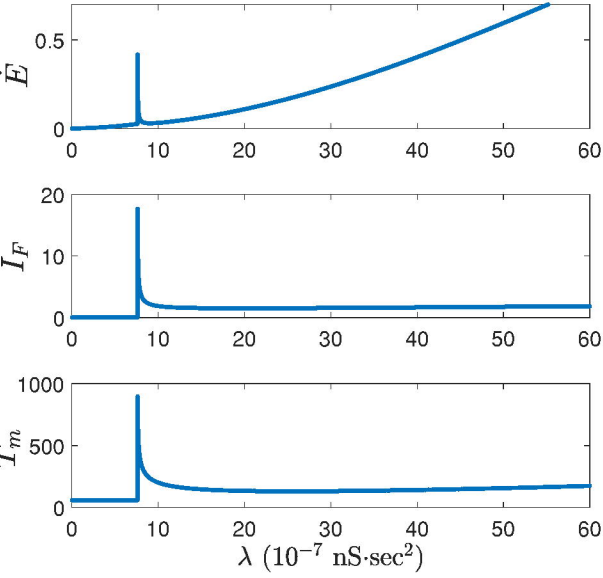
$\dot{E}$
0.5
0
0
10
20
30
40
50
60
I_F
20
10
0
0
10
20
30
40
50
60
T_m
1000
500
0
0
10
20
30
40
50
60
λ (10^{-7} nS·sec^2)

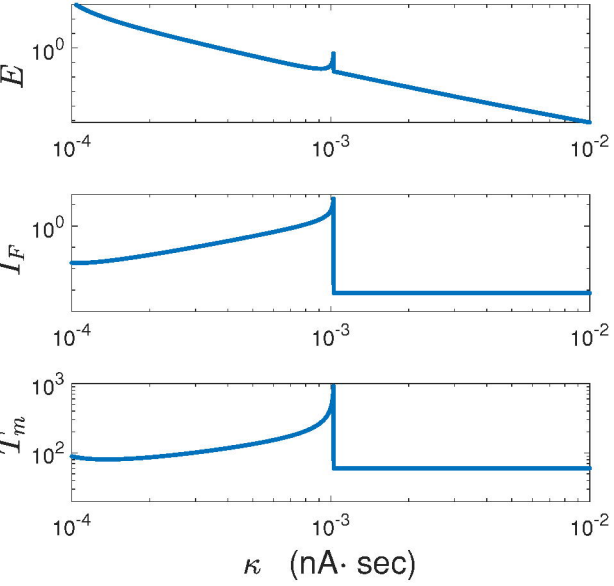
$\dot{E}$
10^0
10^{-4}
10^{-3}
10^{-2}
I_F
10^0
10^{-4}
10^{-3}
10^{-2}
T_m
10^3
10^2
10^{-4}
10^{-3}
10^{-2}
κ (nA· sec)

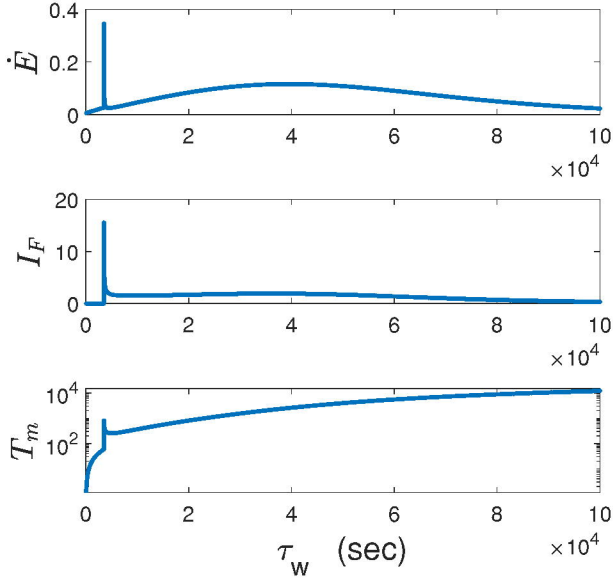
$\dot{E}$
0.4
0.2
0
0
2
4
6
8
10
$\times 10^4$
I_F
20
10
0
0
2
4
6
8
10
$\times 10^4$
T_m
10^4
10^2
0
2
4
6
8
10
$\times 10^4$
τ_w (sec)